



Elisabete Trindade Pedrosa Near-Infrared Spectroscopy for estimating soil burn severity

Thesis submitted to the University of Aveiro to meet the requirements for the degree of Master in Environmental Studies, inserted in the Joint European Master in Environmental Studies (JEMES) program, and elaborated under the scientific guidance of Jan Jacob Keizer, Ph.D., Assistant Researcher at the Centre for the Environmental and Marine Studies (CESAM), Department of Environment and Planning, University of Aveiro, and co-supervision of Antoni Rosell Melé, Ph.D., Professor at the Institute of Environmental Science and Technology (ICTA), Autonomous University of Barcelona.

The Joint European Master in Environmental Studies (JEMES) program is offered by four north European Universities: *Technische Universität Hamburg-Harburg (TUHH)*, Germany; *Universitat Autònoma de Barcelona (UAB)*, Spain; *Universidade de Aveiro (UA)*, Portugal, *Aalborg Universitet (AAU)*, Denmark. An ERASMUS MUNDUS scholarship from the European Union.

the jury

president

Professor Doctor Ana Isabel Couto Neto da Silva Miranda

Aggregate Associate Professor at Department of Environment and Planning,
University of Aveiro

Professor Doctor António José Dinis Ferreira

Associate Professor at Environment and Exact Sciences Department, Superior
Agrarian School of Coimbra

Doctor Jan Jacob Keizer

Assistant Researcher at the Centre for the Environmental and Marine Studies
(CESAM), Department of Environment and Planning, University of Aveiro

acknowledgements

First of all, I want to thank Cesar Guerrero for his time, kindness and patience in passing on his knowledge, even when we didn't always speak the same language.

Thanks also go to my supervisors, Jan Jacob Keizer and Antoni Rosell, for accepting the challenge of giving me the right orientation.

Special thanks are for Alfonso, Esperanza, Sara, Elizabeth, and Uwe for being so kind and trusting literally a stranger in their home, and all the people that supported me, and trusted me during these two years.

I am very thankful to Nadia, Jesus, and Hugo for being the best friends ever, and for reminding me always how to have fun, and for making me happy.

I also want to thank the people that gave me a hard time, because with them I also learned important life lessons.

And last but not least, I thank my mother for being so supportive, comprehensive, and the perfect mum ever.

I gratefully acknowledge the financial support of the project FIRECNUTS (PTDC/AGRCFL/104559/2008), funded by the FCT/MCTES (PIDDAC), with co-funding by FEDER through COMPETE (Programa Operacional Factores de Competitividade; POFC) as well as the contributions by Diana Vieira, Silvia Estrela, and Marifé Varela for their great job in collecting the field samples, without which this study would not have been possible.

Keywords NIR spectroscopy ; soil ; severity ; temperature ; forest wildfires

Abstract Forest fires are a natural phenomenon and occurred long before human kind was around, serving important ecosystem functions. In the past decades, however, some parts of the world have seen marked increases in the frequency and spatial extent of wildfires. This includes Portugal, where forest fires have, on average, affected 100.000 ha of rural lands per year since the mid1970s.

In general, the direct and indirect effects of fires depend strongly on the temperatures to which vegetation and soil are exposed. In the case of wildfires – as opposed to prescribed burning or experimental fires - these temperatures can hardly ever be measured. Therefore, wildfire impacts are commonly assessed using proxies based on the consumption of the vegetation and the colour of the ashes deposited on the soil surface. These so-called burn severity indices typically provide qualitative estimates, distinguishing between low, medium and high severity. Recently, however, near- infrared (NIR) reflectance spectroscopy was successfully applied to estimate the maximum temperatures reached (MTR) by soils heated under laboratory conditions. The present study wanted to explore the potential of NIR for estimating MTR in soils burnt by wildfires. To this end, the work addressed two main topics: (i) spatial variability in the relationships between soil heating temperatures in a muffle and the corresponding NIR-based MTR estimates, both between and within study sites; (ii) the importance of this spatial variability in estimating MTRs of wildfire-burnt soil samples.

A number of NIR-based models was constructed and used to predict the known MTR of laboratory-heated soil samples. One of the two long-unburnt study sites revealed marked variability over short distances, whereas the other did not. The models based on larger sample numbers, however, provided robust MTR predictions, even when these models involved samples from the two study sites. This probably reflected the sites comparable parent materials, soils and land cover (eucalypt plantations in schist soils).

The best achieved models were used to estimate MTR by soil samples from a wildfire occurred in the central-north of Portugal, in the year 2010.. According to the index proposed in this work and the maximum temperatures reached estimations, the soil burn severity of the studied sites was moderate to high in surface samples, and low to moderate in the sub-surface samples.

INDEX

List of Figures	iv
List of Tables	v
Chapter 1 – General introduction	1
1.1 Background	2
1.2 Fire effects on soils	5
1.3 Near-infrared spectroscopy.....	7
1.3.1 Chemical principles.....	7
1.3.2 Model construction and application	8
1.4 Objectives and thesis structure.....	10
Chapter 2 – Near-infrared spectroscopy for determination of (wild-)fire burn severity in soil	13
2.1 Introduction	14
2.2 Materials and methods.....	17
2.2.1 Study area and sites	17
2.2.2 Field sample collection	19
2.2.3 Laboratory Heating Treatments and Temperature Measurements	20
2.2.4 Measurement of near-infrared (NIR) spectra	21
2.2.5 Analytical process of model construction	21
2.2.6 Model assessment based on laboratory-heated soils	23
2.2.7 Model assessment based on wildfire-burnt soils	28
2.2.8 Wildfire soil maximum temperatures Reached (MTR) and burn severity classification	29
2.3 Results and discussion	30
2.3.1 Model assessment based on laboratory-heated soils	30
2.3.2 Model assessment based on wildfire-burnt soils.....	48
2.3.3 Wildfire soil maximum temperatures reached (MTR) assessment and burn severity classification	55
2.4 Conclusions.....	60
Chapter 3 – The applicability of near-infrared spectroscopy in the study of soils.....	61

LIST OF FIGURES

<i>Figure 1 Study area, and sites location</i>	18
<i>Figure 2 Results of the RPD of all model applications, organized by the type of models applied to the ten sampling points of each site. The lines don't indicate continuity of data, but were maintained to facilitate the observation of results.</i>	47
<i>Figure 3 Relation between maximum temperatures reached in the soil samples measured with thermocouple and predicted by near-infrared spectroscopy in the validations of S1 models. Unfiled points denote outliers (not removed)</i>	49
<i>Figure 4 Relation between maximum temperatures reached in the soil samples measured with thermocouple and predicted by near-infrared spectroscopy in the validations of S2 models. Unfiled points denote outliers (not removed)</i>	52
<i>Figure 5 Results of the MTR estimations of site B1 including the standard deviation when more than one model was used for estimation. The unfilled sample was outlier in all MTR estimations.</i>	57
<i>Figure 6 Results of the MTR estimations of site B2 including the standard deviation when more than one model was used for estimation. The unfilled sample was outlier in all estimations (sampling point 7 0-2 cm).</i>	57
<i>Figure 7 Results of the MTR estimations of B3 including the standard deviation when more than one model was used for estimation. The unfilled sample was outlier in all estimations.</i>	58

LIST OF TABLES

<i>Table 1 General characteristics of the study sites.</i>	19
<i>Table 2 Overview of soil samples collected at the burnt and unburned study sites</i>	19
<i>Table 3 Heating treatments of the unburned soil samples.</i>	20
<i>Table 4 Classification and applicability of models defined by the residual predictive deviation (RPD).</i>	24
<i>Table 5 Details of the development of UB1 models with increasing model complexity levels. Each letter corresponds to a sampling point set of samples. MC= model complexity</i>	26
<i>Table 6 Details of the development of UB2 models with increasing model complexity levels. Each letter corresponds to a sampling point set of samples. MC= model complexity</i>	26
<i>Table 7 Details of the development of models UB1, and UB2.</i>	27
<i>Table 8 Details of the development of the two-site or complexity nine models (MC9).</i>	27
<i>Table 9 A burn severity index classification that includes amount of biomass destruction (Indicator 1), mineral soil appearance (Indicator 2), soil properties modifications and maximum temperatures reached.</i>	29
<i>Table 10 Calibration parameters of complexity one models (MC1). n= number of samples (spectra + MTR in the oven) in the data set.</i>	30
<i>Table 11 Results of the application of complexity one models (MC1), for site UB1.</i>	32
<i>Table 12 Calibration parameters of models complexity two (MC2), three (MC3), and four (MC4), of site UB1. n= number of samples (spectra + MTR in the oven) in the data set</i>	33
<i>Table 13 Results of the slope of true versus predicted values, and of the R2 (in %) from the application of models complexity two (MC2), three (MC3) and four (MC4) of site UB1.</i>	34
<i>Table 14 Results of the average RMSEP (in °C) of the MTR predictions plus its standard deviation (when applicable), using models of site UB1. MC= model complexity; n°= number of model applications.</i>	35
<i>Table 15 Results of the average number of outliers (maximum=18) plus its standard deviation (when applicable), of the MTR predictions using UB1 models. MC= model complexity; n°= number of model applications</i>	35
<i>Table 16 Results of the average RPD plus its standard deviation (when applicable), of the MTR predictions using UB1 models. MC= model complexity; n°= number of model applications</i> ...	36
<i>Table 17 Calibration parameters of complexity one models (MC1), of site UB2. n= number of samples (spectra + MTR in the oven) in the data set.</i>	37
<i>Table 18 Results of the application of complexity one models (MC1), of site UB2.</i>	38
<i>Table 19 Calibration parameters of models complexity two (MC2), three (MC3), and four (MC4) of site UB2. n= number of samples (spectra + MTR in the oven) in the data set</i>	39
<i>Table 20 Results of the slope of true versus predicted values, and of the R2 (in %) from the application of models complexity two (MC2), three (MC3) and four (MC4) of site UB2.</i>	40

Table 21 Results of the average RMSEP (in °C) of the MTR predictions plus its standard deviation (when applicable), using models of site UB2. MC= model complexity; n ^o = number of model applications.....	41
Table 22 Results of the average number of outliers (maximum= 18 or 19) plus its standard deviation (when applicable), of the MTR predictions using UB2 models. MC= model complexity; n ^o = number of model applications.....	41
Table 23 Results of the average RPD plus its standard deviation (when applicable), of the MTR predictions using UB2 models. MC= model complexity; n ^o = number of model applications ...	42
Table 24 Calibration parameters of models UB1, and UB2. n= number of samples (spectra + MTR in the oven) in the data set.....	43
Table 25 Results of the application of models UB1 and UB2 to the samples of UB2 and UB1, respectively.....	43
Table 26 Calibration parameters of the two-site or complexity nine models (MC9). n= number of samples (spectra + MTR in the oven) used in the data set.....	44
Table 27 Results of the application of the two-site or complexity nine models (MC9).....	45
Table 28 Results of the MTR estimations (in °C) of site B1 using S1 models. The asterisk denotes outliers.	50
Table 29 Results of the MTR estimations (in °C) of site B2 using S1 models. The asterisk denotes outliers.	50
Table 30 Results of the MTR estimations (in °C) of site B3 using S1 models. The asterisk denotes outliers.	51
Table 31 Results of the MTR estimations (in °C) of site B1 using S2 models. The asterisk denotes outliers.	53
Table 32 Results of the MTR estimations (in °C) of site B2 using S2 models. The asterisk denotes outliers.	54
Table 33 Results of the MTR estimations (in °C) of site B3 using S2 models. The asterisk denotes outliers.	54
Table 34 Comparison of the results of the percentage of outliers in the MTR estimations of both strategies (S1 and S2) discriminated by model and site.	55
Table 35 Results of the assessment based on the standard deviation of the MTR (in °C) estimated by the three models of S1 and S2 for each depth, and the total standard deviation (six models and both sample depths).....	56
Table 36 Classification of the soil burn severity of both surface (0-2 cm depth) and underneath (2-5 cm depth) samples of each wildfire-burnt site (B1, B2, and B3).	59

CHAPTER 1 – GENERAL INTRODUCTION

1.1 BACKGROUND

Forest fires are a natural phenomenon and occurred long before mankind was around (Walter L. and Cressler III, 2001, Bowman et al., 2009), which contributed in conjunction with the climate to the dynamics of flora and vegetation serving important ecosystem functions that made the original earth landscapes (Kelley, 2009). In the last century, human expansion to forested areas, and changes in climate have created a situation where forest wildfires, linked or not to natural causes, can adversely affect lives, propriety, and ecosystems (Nasi et al., 2002).

Portugal is characterized by a Mediterranean climate with a wet winter and a hot and dry summer. The dry season, allied to the accumulation of forest biomass attributed to the abandonment of agricultural land and forestry (Ferreira et al. 2005), has contributed to the increment in the number and magnitude of forest fires. The Portuguese forest area has a high social and economic value to the country, occupying an area (scrubs and stands) of 5,385,187 ha and representing 61% of continental Portugal (IFN5, 2006). In the last decade almost 1.5 million hectares of forested area were burnt (ICNF - Statistics 2001-2010), which represents considerable economic and social losses for the country. After the fire season, more or less heavy rains can reinforce the negative effects of fires (especially erosion and soil degradation). For this reason, it is important to have a fast assessment of the damage right after the fire occurs so as to concentrate resources on high priority areas and target recovery activities efficiently (Miller and Yool, 2002). Thus, the management of burnt areas aims to mitigate adverse ecosystem responses (particularly erosion potential and hydrologic response), and to decrease the recovery time of the ecosystems affected by fire (Miller and Yool, 2002). The terms fire severity and burn severity are often used interchangeably to describe fire-induced damages (Keeley, 2009). To avoid confusion between these two terms, here the term burn severity was considered to be the most appropriate. Kelley (2009) suggested that fire severity should concern measurement of effective changes by fires (e.g. tree crown canopy scorch; ash deposition), whilst burn severity should be applied to soils and restricted to field measurements; the author also argued both these terms should be separated from the definition of ecosystem responses (e.g. erosion processes and vegetation recover).

Lentile et al. (2006) and Veraverbeke et al. (2010) also suggested a distinction between fire and burn severity, taking into account the fire disturbance continuum presented by Jain (2004), which involved four components: pre-fire environment, fire environment, post-fire environment, and the biological and physical response to the environment. Jain et al. (2008) then reformulated this as a cycle linking the first three components. The pre-fire environment includes forest vegetation and state of the environment (moisture levels, amount of biomass, and species composition) immediately prior to the fire as well as during the preceding year. The fire environment includes the characteristics during combustion (e.g. weather, fire behaviour, and suppression tactics), the fire intensity (descriptor of fire behaviour, such as time averaged energy-flux in $W.m^{-2}$) and fire severity (direct fire effects). The post-fire environment includes burn severity (descriptor of what is left after the fire is out and addressing the physical, chemical, and biological properties of the soil), as well as the ecological, social, and economic responses (descriptor of short-to long term, indirect effects).

Burn severity classifications, however, are often based on degree of biomass destruction, and do not include modifications of soil proprieties. When based on fieldwork (e.g. Perez and Moreno, 1998; Lewis et al., 2006), such classifications are labour-intensive, time-consuming and costly and, especially if large areas are involved (De Santis and Chuvieco, 2007). To obtain quick coverage of large areas, remote sensing has been employed to map fire-induced changes in forest structure (such as decrease in vegetation cover and the amount of exposed soil) and vegetation moisture content (e.g. van Wagendonk et al., 2004; Cocke et al., 2005). The lack of information about the specific changes in soil proprieties of these methods risk of under-classifying or over-classifying the wildfire-affected areas, misleading managers when applying emergency rehabilitation treatments (Lewis et al., 2006).

Fire-induced effects on soils depend to a large extent on the temperatures reached (e.g. Raison, 1979; Almendros et al., 1984, 1988, 1990; Ulery y Graham, 1993; Neary et al., 2005; Pietikäinen et al., 2000; Fernández et al., 2001; González-Pérez et al., 2004; Certini, 2005; Guerrero et al., 2005; Marcos et al., 2007; Terefe et al., 2008). Near infrared (NIR) reflectance spectroscopy is a cost-effective, time-saving, non-destructive, and environmentally-sound soil analysis technique (Dunn et al., 2002). Allied to *chemometrics* it has proven to be effective in obtaining reliable estimations of the maximum

temperatures reached (MTR) of lab-burned samples (Guerrero et al., 2007; Arcenegui et al., 2008; Arcenegui et al., 2010), and of prescribed-fire soil samples (Lugassi et al., 2010). The first and, to the best of our knowledge, the only study that employed NIR-based estimates of soil heating by wildfire was Maia et al. (2012). The authors related the post-fire soil seed bank in a Maritime Pine stand with several severity indices, finding a better correlation with the twig index than with the NIR-base MTR. The range of temperatures used for model construction in Maia et al (2012) were between 100°C and 700°C (at a scale of 100°C), and times of burning 10, 20 and 40 minutes, however the MTR estimation results ranged from 53°C to 125°C. Fires tend to move quickly, thus hardly a soil sample will be subjected to peak temperatures during a large amount of time (Molina et al., 2001). This suggests that the model used by Maia et al. (2012) for the MTR predictions could be of low quality, which certainly had a negative impact in the MTR estimations. Considering this, in order to perform a more "realistic" calibration (that mimics reality), in the present work the temperature and times of burning scale at which samples for calibration were subjected was smaller than in the above mentioned studies.

NIR spectroscopy calibrations have not performed well across soil types, smaller or more similar areas have resulted in better predictions for a number of soil properties (Sankey et al., 2008). This is believed to be due to soil mineralogy (Russel, 2003). Thus, one of the main gaps in effective monitoring of soil quality with NIR spectroscopy is the building of NIR-based regression models capable of assessing soil conditions at the global or regional scale across various soil types (Cecillon et al., 2009). Shepherd & Walsh (2002) presented an approach for regional quantification of soil properties with laboratory spectrometry. They proposed the use of soil spectral libraries as a tool for building risk-based approaches to soil evaluation. In the spectral library approach, soil properties are measured conventionally for a selection of soils representative of the diversity of the studied region, and then calibrated to soil reflectance spectra (Cecillon et al., 2009). In this framework, calibrations (models) of the NIR-spectra in function of the MTR can be added to this library. Thereby, coupling both peak temperatures and soil quality information may enable faster assessment of the soil burn severity of a determinate area after a fire event, and better comprehension of the post-fire evolution of different soil proprieties, the response of vegetation, the hydrological changes and erosion processes. Moreover, in

Guerrero et al. (2007) study, the loss of predictions accuracy brought about by including samples that were spectrally and chemically heterogeneous in a global calibration (different soil types) showed that global calibrations are not systematically better than local calibrations and that care must be taken in forming heterogeneous calibration sets, recommending the use of local models (same soil type) instead of global models.

As already mentioned, one advantage of using NIR spectroscopy is to be time-saving. In this sense, the number of samples for laboratory analyses, and data processing (to perform the calibrations) needs to be kept to a minimum. Furthermore, the time frame available for soil spectra to reflect soil temperatures after a fire event can be quite limited, either due to erosion or human activity (Guerrero et al., 2007; Lugassi et al., 2010), thus the number of field samples to be collected need also to be kept to a minimum. However, so that to perform good and trustworthy estimations, models require limited but sufficient heterogeneity, what in this work is referred as variability (Cecillon et al., 2009).

1.2 FIRE EFFECTS ON SOILS

The effects of fire on soils can be positive. Low intensity fires, usually associated to human controlled fires, can increase the productivity of the soil. This happens because the nutrients that were retained in the plant tissue and the organic matter are released to the soil, in a more accessible form to plants, acting as a fertilizer soil. On the other hand, high intensity fires can have quite negative impacts on ecosystem health (Verma and Jayakumar, 2012).

The direct effects of fire on soil proprieties depend mainly on peak temperatures and their duration, but also on aspects such as the resistance of the soil to heating, which possibly varies with soil texture, soil moisture and even up/downslope direction of the fire spreading (Certini, 2005).

The extent and duration of the effects of fire depend on the severity of the fire. They are controlled by several environmental factors that affect the combustion process, such as quantity, nature and moisture of live and dead fuel, air temperature and humidity, wind speed and topography of the site (Certini, 2005). In other hand, the resilience of the burnt

area is dependent on the interaction of many factors, including fire intensity, duration of the fire, vegetation type, climate, slope, topography, soil characteristics, time past since the last fire, and burnt area (Neary et al., 1999). Fire has an impact on the ecosystem services provided by the forest, which can encounter a range of ecological, political, economic, social and cultural considerations and processes such as, livestock, fresh water, wild foods, polinization, or climate regulation from soil carbon sequestration (GFA - FAO, 2010).

Fire affects the physical, chemical and biological properties of soils (Certini, 2005). Important heat-induced soil physical characteristic changes are: colour, texture, pH, bulk density, and water holding capacity (Verma & Jayakumar 2012). The most representative change on chemical proprieties of soil during burning is loss of organic matter (Certini, 2005), having also an impact on macro and micronutrient dynamics. Worth stressing that the soil organic layer provides a protective cover that mitigates erosion, aids in regulating soil temperature, provides habitat and substrates for soil biota and can be major source of readily mineralizable nutrients (Neary et al., 1999). Fire affects soil dwelling invertebrates that play an important role in litter decomposition, C and nutrient mineralization, soil turnover and soil structure formation (Neary et al., 1999). Mycorrhiza and soil bacteria are also affected by fire, the first maintains overall forest health, and the second is important for the ecosystem bio-chemical cycles (Verma & Jayakumar 2012).

In particular, fire can cause partial or complete combustion of organic matter, deterioration of soil structure, modification of the porosity, increased bulk density (e.g. Giovannini et al., 1988; Imeson et al., 1992) altered (usually reduced) aggregate stability (e.g. Llovet et al., 2009; Úbeda and Bernia, 2005), depletion of nutrients through volatilization and convection of ash and smoke columns and through leaching, together with marked alterations of the numbers and composition of soil microbial and soil-dwelling invertebrates (Certini, 2005). Fire may alter (often increasing) the soil water repellence characteristics of a soil (e.g. Doerr et al., 2000, 2006; Coelho et al., 2004), although it can also have little or no impact where this property already exists (e.g. Doerr et al., 2009). Many of these changes potentially make the soil more susceptible to removal by water erosion (e.g. Gabet, 2003; Carroll et al., 2007; Shakesby, 2011) and/or less likely to allow infiltration and more likely to promote overland flow (Wagenbrenner et al., 2006).

Inside Portugal, the increase of runoff and the erosion risk are mainly indicated as post-fire ecosystem responses (e.g. Ferreira et al., 2005; Keizer et al., 2008; Malvar et al., 2011). These effects are attributed to soil degradation and consequent loss of vegetation cover (Ferreira et al., 2008). Some authors suggest that the most disturbing effect on soil degradation is the loss of soil aggregates stability, and water repellence which in turn influences the hydrological response (Coelho et al. 2004; Doerr et al. 2006).

1.3 NEAR-INFRARED SPECTROSCOPY

1.3.1 CHEMICAL PRINCIPLES

Molecular spectroscopy is based in the interaction between electromagnetic radiation and the molecules. According to the spectroscopic phenomenon that is caused by the absorption of energy by matter, the near-infrared is the region between 780 and 2500 nm (wavelength) or between ≈ 12820 and 4000 cm^{-1} (wavenumber) (Sheppard et al., 1985).

As mentioned before, fire has direct effects on the physical, chemical and biological properties of soils (Certini, 2005), that depend to a large extent on the temperature reached by the soil (Raison, 1979). In other words, during a fire soil properties experiment several changes. Each different property undergoes distinct modifications depending on the temperatures reached by the soil. Many of these modifications have a spectral response in NIR, or are properties that can be estimated by NIR (Fritze et al., 1994; Viscarra Rossel et al., 2006, Guerrero et al., 2007; Zornoza et al., 2008; Cecillon et al., 2009; Lugassi et al., 2010).

In the NIR region, the radiation is absorbed by different chemical bonds (mostly C–H, N–H, S–H, C=O, and O–H) depending on its concentration in the sample. The NIR spectra are the result of overtones and band combinations from the fundamental vibrations (Burns and Ciurczak, 2001). As a consequence of the overlapped bands, NIR information has to be extracted and cannot be directly interpreted. To take advantage of the useful information contained in the NIR spectra, sophisticated computer programs that perform multivariate statistics are often used to extract this information (e.g. Martens and Næs,

1989; Burns and Ciurczak, 2001; Næs et al., 2002). Thus, it is possible to construct a model that relates the changes in NIR spectra of soil burnt at different temperatures, and use it to estimate/predict the temperature reached by other soil samples (Guerrero et al., 2007) in a very simple process. First the maximum temperature reached is accurately measured in a set of soil samples (laboratory heating); after this, the NIR spectra of these same samples are obtained. Both sources of information (information matrixes) are then used to construct a calibration matrix (model).

1.3.2 MODEL CONSTRUCTION AND APPLICATION

The calibration process that relates the spectral information with the MTR consists in performing a multiple regression analysis commonly known as, the PLS regression. The PLS regression is the most common method used to perform function calibrations using NIR spectroscopy (Martens and Næs, 1989; Wold et al., 2001; McBratney et al., 2006; Næs et al., 2002; Burns and Ciurczak, 2001; Viscarra Rossel et al., 2006). PLS regression is a multiple regression that uses the PLS vectors (also called latent variables) as predictor variables (or independent variables). Thus, in the calibration process, the calibration function (adjusted by the least squares) that relates the spectra with the MTR is constituted by PLS vectors that have the same dimension of the spectra. Depending on the number of PLS vectors included in the calibration function, the model will have distinct rank. It is preferable to use lower rank in the model, because the higher the number of PLS vectors, less new information, and more "noise" is being added to the models. The overfitting (too high rank) can have negative effects when performing the estimates (Næs et al., 2002), on the other hand if an underfitting occurs, the information added to the calibration function can be insufficient, losing the ability to relate the data. To decide which is the best rank to be used in the model, it is useful to analyze the sedimentation graphs that represent the evolution of both r^2 , and RMSECV (root mean square error of the cross validation) with the rank (number of PLS vectors). Theoretically, as the rank increases, also increases the quality of the fit (r^2) and the error is reduced. At some point

when the adjustment increase and the decrease of the error are almost negligible, it is not worth to use more PLS vectors.

In addition to the information of the chemical composition, a spectrum also contains some information on certain physical properties of the sample; the particle size, the density, and the compaction of the sample are among the main factors that are also recorded in the spectrum (Burns and Ciurczak, 2001). Therefore, it is common to apply one or more preprocessing to the spectra before its analysis and interpretation (Blanco and Villarroya, 2002), that in most cases, aiming to find the relationship between spectra and chemical composition, facilitate the calibration process (Naes et al., 2002). Typical spectroscopic preprocessing are, namely, first derivate, second derivate, linear offset subtraction, straight line subtraction, multiplicative scatter correction, vector normalization, min-max normalization.

Once having the calibration function (model), the prediction (or estimation) process is relatively simple. The only need is to apply the calibration function to the spectra of the samples to be estimated (or predicted), applying also the same preprocessing algorithm used in the calibration. Before predicting the dependent variable (in this case the maximum temperature reached), it is important to verify if the model is sufficiently representative of the samples to be predicted. In this sense, a projection of the spectra samples to be predicted can be made, in the spectral space of the model. The easiest way is to use the spectral space generated by the first principal components, although the most effective is to use statistical parameters such as the *Mahalanobis* distance. With this parameter, it is possible to identify if the spectrum of the samples is within the model domain, and therefore have an estimate of whether the prediction has a good quality or not. Thus, this distance offers a way of measuring the reliability of the prediction. The estimations in samples that have high *Mahalanobis* distance may be of low quality, and probably incorrect (Martens and Naes, 1989, Naes et al., 2002, Guerrero et al. 2007). In consequence, statistical packages often include an outlier analysis, based on this distance. When a model is developed, a spectral space is generated, and for a sample to be correctly estimated, it should be inside this spectral space. Sample spectra that are very distinct from those used in the model, remain poorly represented in the spectral space, thus the quality of the prediction is low. As with any type of model, working outside the limits of the model can result in erroneous or imprecise estimates.

1.4 OBJECTIVES AND THESIS STRUCTURE

This work wants to contribute to a better knowledge of the use of NIR reflectance spectroscopy as an alternative and/or complementary tool for estimating burn severity at a local to regional scale, having the potential of providing quantitative estimations of wildfire-induced soil heating. It is divided in two essential parts. The research questions addressed here were:

- Can a single sample from a single spot at one specific study site be representative of other spots on the same site and/or to spots on other sites that have the same soil type? Or in other words, how many samples are necessary to have a representative set of spectra for a given soil type, to construct a model that gives reliable predictions or estimations?;
- Regarding MTR estimations of wildfire-burnt soil samples one cannot easily validate the estimations; however, can a representative and well-calibrated model, overcome the need for validation for wildfire-burnt soils, typically lacking independent temperature estimates?

The two research questions involved different approaches. In the first approach, models were constructed to predict the - known - MTR of laboratory-heated samples, so that the accuracy of the predictions could be used to quantify model performance against spatial variability in soil properties, both within as between study sites. In the second approach, models were constructed to estimate the – unknown – MTR of wildfire-burnt samples (to avoid confusion, a distinction is made here between prediction of known MTR and estimation of unknown MTR). Since the accuracy of the MTR estimates cannot be determined, the performance of the models was assessed in a qualitative manner based on the *Mahalanobis* distance, which offers a way of measuring the reliability of the estimations. The estimations in samples that have high *Mahalanobis* distance may be of low quality, and probably incorrect (Martens and Naes, 1989, Naes et al., 2002, Guerrero et al. 2007).

The specific objectives and were the following:

A. Model assessment based on laboratory-burnt soils

A1. Within-site variability

- to assess the NIR-identified soil variability within each of two unburnt study sites;
- to assess the accuracy of the predicted maximum temperatures reached (MTR) for models based on increasing number of samples.

A2. Between-site variability

- to assess the accuracy of a model developed from samples of one study site to predict the MTR of the oven-heated samples of the other study site (both sites having similar soil sand land cover);
- to assess the accuracy of models developed from samples of both study sites.

B. Model assessment based on wildfire-burnt soils

B1. Strategy 1

- to assess the response of NIR-based models constructed from the laboratory-heating data of the two unburnt study sites separately as well as together

B2. Strategy 2

- To assess the quality of response of NIR-based models with different ranks, since overfitting of a model can negatively affect estimates (Næs et al., 2002).

With these objectives, this first chapter of this thesis includes: the framework of this work; a brief resume of fire effects on soils; the applicability of NIR reflectance spectroscopy in the study of soils and its chemical principles; and the general technique used in model construction and its application.

The second chapter, written in scientific paper format, begins with an introduction based on all information given in the first chapter. Then a detailed description of all materials and methods is made, which includes: the description of the study area and sites; the field

sample collection; all the laboratory and analytical process of analysis; the methodology used in both model assessment approaches; and the description of how the best MTR estimations were selected and classified in terms of burn severity. Then all results and its discussion are exposed. This chapter ends with the main conclusions achieved.

The thesis ends in the third chapter, which refers to the applicability of near-infrared spectroscopy in the study of soils and its link to this work.

A list of the bibliographic references used in this document is also presented.

**CHAPTER 2 – NEAR-INFRARED SPECTROSCOPY FOR DETERMINATION
OF (WILD-)FIRE BURN SEVERITY IN SOIL**

2.1 INTRODUCTION

Forest fires are a natural phenomenon, and occurred long before mankind was around (Walter L. and Cressler III, 2001, Bowman et al., 2009). In conjunction with climate, they played a key role in the dynamics and evolution of flora and vegetation and served important ecosystem functions in the original earth landscapes (Kelley, 2009). In the last century, human expansion of forested areas together with changes in climate have created a situation in which forest wildfires, whether directly linked to human causes or not, can adversely affect human lives, propriety, and (semi-)natural ecosystems (Nasi et al., 2002). In present-day Portugal, wildfires occur frequently and affect large areas, amounting to almost 1.5 million ha in the last decade (ICNF - statistics 2001-2010) and representing significant social and economic losses.

Fire directly affects the physical, chemical and biological properties of soils (Certini, 2005). Important heat-induced changes in soil physical characteristics include colour, texture, pH, bulk density, and water holding capacity (Verma & Jayakumar 2012). The most commonly observed change in soil chemical properties is that in organic matter (Certini, 2005), with direct consequences for the macro- and micro-nutrient stocks and dynamics. The (partial) consumption of the litter layer is particularly relevant, as it provides a protective cover that mitigates erosion, regulates soil temperature, is habitat to soil biota and often is major source of readily mineralizable nutrients (Neary et al., 1999). Soil biological organisms affected by fires include soil bacteria, mycorrhiza, seeds and soil dwelling invertebrates. The former, for example, are especially important for the ecosystem's bio-chemical cycles (Verma & Jayakumar 2012), whilst the latter are crucial in litter decomposition, C and nutrient mineralization, soil turnover and soil structure formation (Neary et al., 1999).

The effects of fire on soil properties depend to a large extent on the temperatures reached (Raison, 1979; Almendros et al., 1984, 1988, 1990; Ulery y Graham, 1993; Neary et al., 2005; Pietikäinen et al., 2000; Fernández et al., 2001; González-Pérez et al., 2004; Certini, 2005; Guerrero et al., 2005; Marcos et al., 2007; Terefe et al., 2008). Soil temperatures during wildfires, however, are difficult to measure. NIR spectroscopy, allied to *chemometrics*, has an elevated potential to overcome this lack of quantitative data on wildfire-induced soil heating. It has allowed to reliably estimate maximum temperatures

reached (MTR), both by soils heated under laboratory conditions (Guerrero et al., 2007; Arcenegui et al., 2008; Arcenegui et al., 2010), and by prescribed-fires (Lugassi et al., 2010). NIR reflectance spectroscopy is also a cost- and time-effective, non-destructive, and environmentally-sound technique (Dunn et al., 2002). The NIR spectra result from the absorbance of radiation in the wavelength region of 780 to 2500 nm ($\approx 12820\text{--}4000\text{ cm}^{-1}$ in wavenumbers) in accordance with the concentration of various chemical bonds, such as C–H, N–H, S–H, C=O and O–H (Burns and Ciurczak, 2001). NIR spectra are dominated by weak overtones and combinations of fundamental vibrational bands of chemical bonds from the mid-infrared region, so that their quantitative analysis requires *chemometrics* (a special branch of multivariate statistics (Burns and Ciurczak, 2001)).

To the best of our knowledge, Maia et al. (2012) was the first and, so far only study that employed NIR reflectance spectroscopy to estimate soil heating by wildfire. The authors related the post-fire soil seed bank in a Maritime Pine stand with several severity indices, finding a better correlation with the minimum twig diameter index than with the NIR-based MTR. Possibly, the model constructed and applied in Maia et al. (2012) was not optimal for the studied burn severities, so that the estimated MTR could be inaccurate. Namely, model construction in Maia et al (2012) involved a wide range of temperatures from 100 °C to 700 °C - and large intervals of 100 °C , whilst the estimated MTR varied from 53 °C to 125 °C. Perhaps also the times of heating in the muffle - 10, 20 and 40 minutes - were not very realistic. Since fires tend to move quickly, peak temperatures attained by soils expectedly are of short duration (Molina et al., 2001). As a follow-up study of Maia et al. (2012), these limitations were explicitly addressed in the present work.

NIR spectroscopy calibrations have not performed particularly well across soil types, smaller or more similar areas have resulted in better predictions for a number of soil properties (Sankey et al., 2008). This is believed to relate to differences in soil mineralogy (Russel, 2003). One of the main gaps for NIR-based monitoring of soil quality is the need for models that are suitable for predicting/estimating soil conditions at the regional or global scale, encompassing a wide variety of soil types and conditions (Cecillon et al., 2009). Nonetheless, Guerrero et al. (2007) found that the accuracy of non-local models (with different soil types) decreased when adding samples with distinct spectral and chemical properties. This demonstrated that non-local models are not necessarily better than local models, so that Guerrero et al. (2007) recommended soil type-specific models.

This work wants to contribute to a better knowledge of the use of NIR reflectance spectroscopy as an alternative and/or complementary tool for estimating burn severity at a local to regional scale, having the potential of providing quantitative estimations of wildfire-induced soil heating. It is divided in two essential parts. The research questions addressed here were: (1a) can a single sample from a single spot at one specific study site be representative of other spots on the same site and/or to spots on other sites that have the same soil type?; (1b) or in other words, how many samples are necessary to have a representative set of spectra for a given soil type, to construct a model that gives reliable predictions or estimations?; (2) Regarding MTR estimations of wildfire-burnt soil samples one cannot easily validate the estimations; however, can a representative and well-calibrated model, overcome the need for validation for wildfire-burnt soils, typically lacking independent temperature estimates?

The two research questions involved different approaches. In the first approach, models were constructed to predict the - known - MTR of laboratory-heated samples, so that the accuracy of the predictions could be used to quantify model performance against spatial variability in soil properties, both within as between study sites. In the second approach, models were constructed to estimate the – unknown – MTR of wildfire-burnt samples (to avoid confusion, a distinction is made here between prediction of known MTR and estimation of unknown MTR). Since the accuracy of the MTR estimates cannot be determined, the performance of the models was assessed in a qualitative manner based on the *Mahalanobis* distance, which offers a way of measuring the reliability of the estimations. The estimations in samples that have high *Mahalanobis* distance may be of low quality, and probably incorrect (Martens and Naes, 1989, Naes et al., 2002, Guerrero et al. 2007).

The specific objectives and were the following:

A. Model assessment based on laboratory-burnt soils

A1. Within-site variability

- to assess the NIR-identified soil variability within each of two unburnt study sites;

- to assess the accuracy of the predicted maximum temperatures reached (MTR) for models based on increasing number of samples.

A2. Between-site variability

- to assess the accuracy of a model developed from samples of one study site to predict the MTR of the oven-heated samples of the other study site (both sites having similar soil sand land cover);

- to assess the accuracy of models developed from samples of both study sites.

B. Model assessment based on wildfire-burnt soils

B1. Strategy 1

- to assess the response of NIR-based models constructed from the laboratory-heating data of the two unburnt study sites separately as well as together

B2. Strategy 2

- to assess the quality of response of NIR-based models with different ranks, since overfitting of a model can negatively affect estimates (Næs et al., 2002).

2.2 MATERIALS AND METHODS

2.2.1 STUDY AREA AND SITES

The study area was located in a small town called Ermida, in Sever do Vouga Municipality (40°43'N, 8°20'O), Aveiro District, north-central Portugal (Figure 1). The area was affected by a wildfire on 26 of July 2010. The fire consumed 295 ha of forest lands (AFN, 2010), mainly plantations of eucalypt (*Eucalyptus globulus*).

The climate of the area is meso-thermal (temperate) humid with a dry season in the summer, which is moderately warm but long (classified as CSb, Köppen (1936) - DRA - Center, 2002). The average annual temperature is 14.9°C, while the monthly averages range from 9.0°C in January and 21.1°C in June (SNIRH, 2011: station Borgães Castle Dam, 13 km north of the study area, 306 m altitude; 1990-2010). (The average annual

rainfall is 1609 mm, and varies between 960 and 2530 mm (SNIRH, 2011: precipitation station of Ribeiradio, located 4.5 km east of the study area and 228 m altitude).

The soils of the study area are predominantly Cambisols and Leptsols (WRB, 2006). They have a coarse texture and are developed over schist.

Five different hill slopes were selected for this study, three of which located within the burnt area (B1, B2, B3) and two in its immediate surroundings to the north-east (UB1 and UB2) (Figure 1). The general characteristics of the five study sites are given in Table 1; all five sites were planted with eucalypt (*Eucalyptus globulus*).

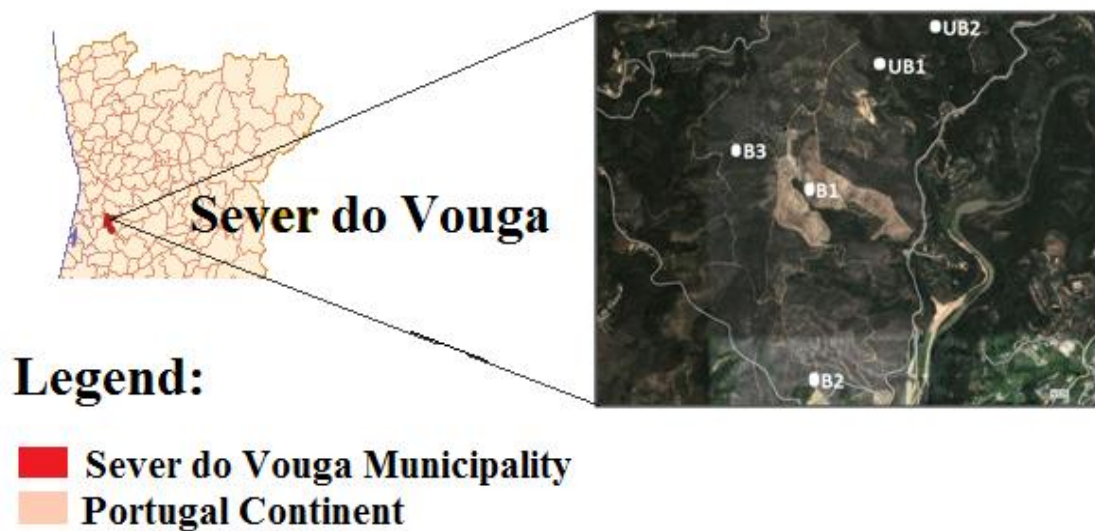


Figure 1 Study area, and sites location

Table 1 General characteristics of the study sites.

Site (code)	Altitude (m)	Orientation	Slope (°)
B1	240	SE	17
B2	140	SE	19
B3	260	SW	24
UB1	230	SE	25
UB2	230	SE	25

2.2.2 FIELD SAMPLE COLLECTION

Unburned samples were collected one month after the fire event. At both sites, five samples were collected at 0-5 cm depth (Table 2). The five sampling points were separated by a few meters along a transect from the base to the top of the hill slope (sites).

Sampling at the burnt sites was done 11 days after the fire event, before the occurrence of any precipitation event. Samples were collected at 0-2 and 2 to 5 cm depth) at 5 or 10 equidistant locations along transects from the the base to the top of the hill slopes Table 2).

All samples were collected using a metal cylinder with a diameter of 6 cm, carefully excluding the ash layer. Prior to storage, the samples were air dried and sieved at a mesh width of 2 mm.

Table 2 Overview of soil samples collected at the burnt and unburned study sites

Study sites codes	Geology parent rock	Sampling points n ^o	Sampling depth(s) cm	Samples n ^o	Sampling points sub-codes
Unburnt sites (UB)					
UB1	Schist	5	0-5	5	a; b; c; d; e
UB2	Schist	5	0-5	5	f; g; h; i; j
Burnt sites (B)					
B1	Schist	5	0-2; 2-5	10	I; II; III; IV; V
B2	Schist	10	0-2; 2-5	20	1; 2; 3; (...); 10
B3	Schist	5	0-2; 2-5	10	α; β; γ; δ; ε

2.2.3 LABORATORY HEATING TREATMENTS AND TEMPERATURE MEASUREMENTS

Since it is widely accepted that soil properties are not only affected by the temperature level, but also by the duration of heating (e.g. Certini, 2005; Lugassi et al., 2010), the unburnt soils were subjected to a range of laboratory controlled heating treatments at different temperatures and times of heating (Table 3).

Table 3 Heating treatments of the unburned soil samples.

	Oven temperature (°C)					
	100	175	250	325	400	500
Time (min)	1	1	1	1	1	1
	5	5	5	5	5	5
	10	10	10	10	10	-

**An extra burn was made to the soil sample point "UB2-f" at 125°C, during 5 minutes.*

In total 171 heating experiments were carried out, using a standard procedure. A furnace-oven (Nabertherm, P320, Bremen, Germany) was pre-heated to the desired temperature before a small quantity of unburnt soil was distributed homogeneously on a plate, to which two thermocouples were attached (k-type, NiCr–Ni; Testo SA, Barcelona, Spain). The soil was placed such that thermocouples slightly touched it. The sample plus thermocouples was inserted inside the oven for the desired time, with the thermocouples recording the temperature at intervals of 3 seconds. The maximum temperature reached (MTR) by the soil sample was then calculated as the average of the maximum temperatures registered by the two thermocouples.

2.2.4 MEASUREMENT OF NEAR-INFRARED (NIR) SPECTRA

The NIR spectra were measured by transferring, the – cooled – laboratory-heated and wildfire-burnt samples to open glass vials (2x5 cm, ~4 g of soil) and then scanning them in reflectance mode from wavenumbers 12000 to 3800 cm^{-1} (approximately equivalent to wavelengths 830 to 2630 nm). This was done using a Fourier-Transform Near-Infrared (FT-NIR) spectrophotometer (MPA; Bruker Optik GmbH, Germany) equipped with a quartz beamsplitter, a PbS detector and an integrating macro-sample sphere. Each of the reflectance measurements involved 64 scans that were then averaged, whereas background corrections were made regularly. Each spectral measurement took approximately 1 min and resulted in a spectrum composed of 2126 values of absorbance (as derived from reflectance values). This was repeated twice for each sample to increase the surface area scanned and the final spectrum was computed as the average of the two repetitions. In total, 221 spectra were obtained, i.e. 85 and 86 from the UB1 and UB2 laboratory-heated samples, respectively; and 50 spectra from the samples collected in the field at the unburnt UB1 and UB2 sites and the wildfire-burnt B1, B2 and B3 sites (see Table 2).

2.2.5 ANALYTICAL PROCESS OF MODEL CONSTRUCTION

All models were developed following Guerrero et al. (2007). All empirical models (calibration functions) were had the following general structure:

$$Y = bX \quad [1]$$

were: Y is the target parameter (MTR), b is the calibration function and X is the NIR spectra, so that:

$$\text{MTR} = b\text{NIR} \quad [2]$$

Thus, two matrixes were constructed:

- the NIR-spectra matrix, composed of n rows (one per sample) and 2126 columns (one per each of the 2126 absorbance values between 830 and 2630 nm).
- the MTR matrix, composed of n rows (one per sample), and one column with the data of MTR in each lab-burned soil sample.

The empirical calibration function b , was determined using partial least squares (PLS) regression. In resume, PLS regression reduces the NIR matrix to a few components or vectors (similar to as is done in principal component analysis) that account best for the measured MTR. The number of PLS components (the rank of the model) should neither be too small nor too large to avoid under- or overfitting of the model. Equation [2] can now be described more accurately as:

$$\text{MTR} = \text{first-PLS-v}(\text{NIR}_{\lambda_x-\lambda_y}) + \text{second-PLS-v}(\text{NIR}_{\lambda_x-\lambda_y}) + \dots + \text{k-PLS-v}(\text{NIR}_{\lambda_x-\lambda_y}) \quad [3]$$

were "PLS-v" are partial least square vectors, " $\text{NIR}_{\lambda_x-\lambda_y}$ " is the region of the NIR spectra related to the MTR, and "k" is the rank of the model or, in other words, the number of PLS-vectors.

Models were constructed using the leave-one-out cross-validation method. With this method, $n-1$ samples are used for calibration, while the excluded sample is estimated (and validated) with the others. This exclusion-step was repeated successively until all samples were validated with calibrations performed by the others.

The model construction was carried out with the spectroscopic software OPUS 5.5 (Bruker Optik GmbH, 2004). This software has an optimization function that automatically calculates calibration functions by using combinations of predefined frequency regions and data preprocessing methods. The result of the optimization run is a list showing the Rank (number of PLS vectors used in the calibration) and the root mean square error of cross validation (RMSECV) value for each combination of predefined frequency regions and data preprocessing methods. However, on the basis of the optimization results the

user needs to find out which the combination yields the best result, and afterwards, perform the validation of the selected calibration. In this case, best calibrations were selected that presented the lowest values of the RMSECV.

2.2.6 MODEL ASSESSMENT BASED ON LABORATORY-HEATED SOILS

According to the objectives, this part of the study aimed to assess the NIR-based models response to within-site, and between-sites variability. As mentioned before, the selected models were the ones that presented the lower values of the root mean square error of cross validation (RMSECV). The rank was pre-established not to be more than 5. The preprocessing chosen was the first derivate coupled with vector normalization, because it resulted in better calibrations.

To assess the accuracy of the MTR predictions, two parameters were used: the root mean square error of prediction (RMSEP) and the number of MTR predictions that appeared as outliers of the model used. The RMSEP and the RMSECV have the same formula:

$$RMSECV = RMSEP = \sqrt{\frac{1}{n} \sum_{i=1}^n (Diff\ i)^2} \quad [4]$$

$$Diff\ i = Ti_{measured} - Ti_{predicted} \quad [5]$$

However, the RMSECV is a measure of the model error (just like an error of the fitting), and the RMSEP is the error calculated after applying the model to a set of samples in which the MTR is known (i.e. the error obtained when the model is applied to those samples for prediction). Lower RMSEP values indicate higher assertiveness of the MTR predictions.

When a model is developed, a spectral space is generated, and for a sample to be correctly estimated or predicted, it should be inside this spectral space. If the model is not sufficiently representative of the predicted or estimated sample, it will appear as an outlier of the model. The OPUS 5.5 software already includes an outlier analysis; based in the

Mahalanobis distance it offers a way of measuring the reliability of the estimation or prediction. The estimations or predictions in samples that have high *Mahalanobis* distance appear as outliers of the model. These may be of low quality and probably incorrect (Martens and Naes, 1989, Naes et al., 2002).

With the aim of comparing the accuracy of our models with other NIR models cited in the literature, the residual predictive deviation (RPD), also named ratio to prediction of deviation, or regression point displacement was calculated. The RPD is the ratio of the standard deviation of the reference data (in this case the MTR in the oven) to the root mean square error of cross validation (RMSECV), providing a basis for standardizing the RMSECV, or the RMSEP (Williams and Sobering, 1993), however its classification is not standardized. According to some authors that use this technique of soil analysis (Chang et al., 2001; Dunn et al., 2002) RPD values higher than 2 can be considered acceptable models, and RPD values higher than 5 can be considered as excellent (Malley et al., 1999). Concerning the applicability of the calibrations using near-infrared reflectance spectroscopy some authors (e.g. Natsuga and Kawamura, 2006) use the RPD classification as defined in Table 4, which was also used in the present study.

Table 4 Classification and applicability of models defined by the residual predictive deviation (RPD).

RPD	Class	Application
0 - 2,3	Very poor	Not recommended
2,4 - 3,0	Poor	Rough screening
3,1 - 4,9	Fair	Screening
5,0 - 6,4	Good	Quality control
6,5 - 8,0	Very good	Process control
8,1 +	Excellent	Any application

The methodologies used for accomplishing the specific objectives of this part of the study are presented next.

2.2.6.1 Within-site analysis

1. To assess the NIR-identified soil variability inside each unburned site (UB1 and UB2), models that represent each sampling point were constructed. These models are referred to as models complexity 1 (MC1). Each model was used to predict the known maximum temperatures reached (MTR) in the oven by the set of samples of its correspondent site (UB1 or UB2).
2. To assess the accuracy of the MTR predictions using models with increasing complexity, models with successive increase in data were constructed, namely, MC2, MC3, and MC4:
 - MC2 - are models that contain the data sets (MTR in the oven + spectra) from two sampling points, and were used to predict the MTR by the other three sampling points site that were not included in its calibration;
 - MC3 - are models that contain the data sets (MTR in the oven + spectra) from three sampling points and were used to predict the MTR by the other two sampling points not included in its calibration;
 - MC4 - are models that contain the data sets (MTR in the oven + spectra) from four sampling points and were used to predict the MTR by the set of samples of the sampling point not included in its calibration.

The methodology used in the in-site analysis is represented in Tables 5 and 6.

Table 5 Details of the development of UB1 models with increscent model complexity levels. Each letter corresponds to a sampling point set of samples. MC= model complexity

MC1		MC2		MC3		MC4	
Model	Used to predict	Model	Used to predict	Model	Used to predict	Model	Used to predict
a	b ; c ; d ; e	a & b	c ; d ; e	a & b & c	d ; e	a & b & c & d	e
b	a ; c ; d ; e	a & c	b ; e ; d	a & b & d	c ; e	a & b & c & e	d
c	a ; b ; d ; e	a & d	b ; c ; e	a & b & e	c ; d	a & b & d & e	c
d	a ; b ; c ; e	a & e	b ; c ; d	a & c & d	b ; e	a & c & d & e	b
e	a ; b ; c ; d	b & c	a ; d ; e	a & c & e	b ; d	b & c & d & e	a
		b & d	a ; c ; e	a & d & e	b ; c		
		b & e	a ; c : d	b & c & d	a ; e		
		c & d	a ; b ; e	b & c & e	a ; d		
		c & e	a ; b ; d	b & d & e	a ; c		
		d & e	a ; b ; c	c & d & e	a ; b		

Table 6 Details of the development of UB2 models with increscent model complexity levels. Each letter corresponds to a sampling point set of samples. MC= model complexity

MC1		MC2		MC3		MC4	
Model	Used to predict	Model	Used to predict	Model	Used to predict	Model	Used to predict
f	g ; h ; i ; j	f & g	h ; i ; j	f & g & h	i ; j	f & g & h & i	j
g	f ; h ; i ; j	f & h	g ; i ; j	f & g & i	h ; j	f & g & h & j	i
h	f ; g ; i ; j	f & g	h ; i ; j	f & g & j	h ; i	f & g & i & j	h
i	f ; g ; h ; j	f & j	g ; h ; i	f & h & i	g ; j	f & h & i & j	g
j	f ; g ; h ; i	g & h	f ; i ; j	f & h & j	g ; i	g & h & i & j	f
		g & i	f ; h ; j	f & i & j	g ; h		
		g & j	f ; h : i	g & h & i	f ; j		
		g & h	f ; i ; j	g & h & j	f ; i		
		g & i	f ; h ; j	g & i & j	f ; h		
		i & j	f ; g ; h	h & i & j	f ; g		

2.2.6.2 Between-site analysis

1. To assess the capability of the model from one site to predict the known MTR in the oven of the other site two models were constructed. One, using all set of samples from site UB1 and the other using all samples from site UB2. Model UB1 was used to predict the maximum temperatures reached (MTR) in the oven by the samples of UB2, and model UB2 was used to predict the MTR in the oven by UB1 samples (Table 7).

Table 7 Details of the development of models UB1, and UB2.

Model code (sampling points)	Used to predict sampling points
UB1 (a & b & c & d & e)	f ; g ; h ; i ; j
UB2 (f & g & h & i & j)	a ; b ; c ; d ; e

2. To assess the accuracy of the MTR predictions using models which include data from both sites, models using the data of both sampling points (UB1 and UB2) were constructed. These two-site or complexity nine models (MC9) were constructed using the data of nine of the ten sampling point data sets of both sites, and were applied to the samples of the sampling point not included in each model (Table 8).

Table 8 Details of the development of the two-site or complexity nine models (MC9).

Model with sampling points	Used to predict sampling points
UB1 (b & c & d & e) & UB2 (f & g & h & i & j)	a
UB1 (a & c & d & e) & UB2 (f & g & h & i & j)	b
UB1 (a & b & d & e) & UB2 (f & g & h & i & j)	c
UB1 (a & b & c & e) & UB2 (f & g & h & i & j)	d
UB1 (a & b & c & d) & UB2 (f & g & h & i & j)	e
UB1 (a & b & c & d & e) & UB2 (g & h & i & j)	f
UB1 (a & b & c & d & e) & UB2 (f & h & i & j)	g
UB1 (a & b & c & d & e) & UB2 (f & g & i & j)	h
UB1 (a & b & c & d & e) & UB2 (f & g & h & j)	i
UB1 (a & b & c & d & e) & UB2 (f & g & h & i)	j

2.2.7 MODEL ASSESSMENT BASED ON WILDFIRE-BURNT SOILS

According to the objectives, in this part of the study models were constructed to estimate the maximum temperatures reached by the wildfire-burnt samples.

To assess the accuracy of the MTR estimations, two parameters were used: the n^o of outliers of the MTR estimations, and the comparison of the depth sample results. Better MTR estimations are considered to be the ones that contain less number of outliers in the estimates, and that discriminate the samples by depth (surface samples are expected to present higher temperatures).

As described before, two strategies were used in the construction of models, namely strategy one (S1) and strategy two (S2):

2.2.7.1 Strategy 1 (S1)

Three models were constructed, namely UB1', UB2' and UB1+UB2', which included respectively all data (spectra + MTR in the oven) from site UB1, all data from site UB2, and the data of both sites. Such as in the previous part, the program (OPUS 5.5) "chooses" the rank (number of PLS-vectors) which results in the best correlation (lowest values of RMSECV, and higher values of r^2), however it was pre-established not to be more than 10. The preprocessing chosen was the first derivate coupled with vector normalization, because it resulted in better calibrations. The three models were then used to estimate the MTR of the wildfire-burnt samples, namely of sites B1, B2, and B3.

2.2.7.2 Strategy 2 (S2)

The same three models were recalibrated (using the same data) as in S1, reducing the rank of the models (the number of PLS-vectors used in the calibration). Lowering the rank of the calibration results in a diminishment of the model fit, reducing the r^2 , and hence increases the value of the RMSECV. Therefore, to avoid also underfitting problems the rank of the models was only reduced until the effect on the r^2 was not too high. Accordingly, the value of the r^2 was limited to be not lower than 90%. The three models, namely UB1", UB2" and UB1+UB2", were then used to estimate the MTR of the wildfire-burnt samples (sites B1, B2, and B3).

2.2.8 WILDFIRE SOIL MAXIMUM TEMPERATURES REACHED (MTR) AND BURN SEVERITY CLASSIFICATION

In this part of the study, the MTR estimations of the models from Strategy 1 (S1), and Strategy 2 (S2) were compared first in terms of the amount of outliers, and secondly by calculating the standard deviation of MTR estimation results. In the selection of the best models was considered as criterion for exclusion, the ones that presented more 50% of outliers in each the wildfire-burnt site estimations. Finally, each sample was given a burn severity classification based on a burn severity index that was build based on Neary et al., (2005) and Jain et al. (2008) articles, and presented in Table 9.

Table 9 A burn severity index classification that includes amount of biomass destruction (Indicator 1), mineral soil appearance (Indicator 2), soil proprieties modifications and maximum temperatures reached.

Indicator 1	Indicator 2	Can favour, or lead to:	MTR °C	Burn severity level	Classification
Unburned	No evidence of recent fire	Presence of seeds (depends on soil humidity)	< 40	0	Unburned
>40% litter cover and/or root mat	Both charred litter and unburned litter could be present		40 - 100	1	Low
	Plurality of black char	Microorganisms death	100 - 200	2	
2% through 39% litter cover and/or root mat	Plurality of gray and/or white char	Water repellence	200 - 300	3	Moderate
		Organic matter destruction			
1% litter cover or root mat	Plurality of black char	Nitrogen volatilization and mineralization with consequent increase of nutrients (e.g. S, Na ⁺ , K ⁺ , P)	300 - 400	4	
		Microbial carbon loss			
	Plurality of gray and/or white char	Water repellence destruction	400 - 500	5	
	Plurality of orange char	Soil mineralogy change	> 500	6	Very high

2.3 RESULTS AND DISCUSSION

2.3.1 MODEL ASSESSMENT BASED ON LABORATORY-HEATED SOILS

The leave-one-out cross validation process was used to evaluate the prediction capability of all NIR-based models. In this section, first the results of the in-site analysis of site UB1 and site B are presented, which includes results of the calibration process (model construction), and the applications to the known maximum temperatures reached (MTR) in the oven. Then the results of the between-site analysis is presented, which also includes both calibration and application of the models. The classification used in the validation of all models was based on the RPD value.

2.3.1.1 Within-site analysis

Site UB1

1. To assess the NIR-identified soil variability of site UB1, models complexity one (MC1) were constructed using the set of samples of each sampling point of UB1. Concerning the calibration of these models (MC1), the values of the R^2 (fit) ranged from 94.18 to 98.76%, the RMSECV ranged from 17.2 to 36.6°C, the ranks of the PLS regression ranged from 3 to 5, and the RPD ranged from 4.1 to 8.8 (Table 10). Even using a small number of samples in the data set ($n=18$), fair to excellent validation parameters were achieved. The number of outliers of the models ranged from 0 to 2 (not removed).

Table 10 Calibration parameters of complexity one models (MC1). n = number of samples (spectra + MTR in the oven) in the data set.

Site code	Model code	Data n	R^2 %	RMSECV °C	Rank	RPD	Class
UB1	a	18	94.18	36.6	3	4.1	Fair
	b	18	97.89	20.9	4	6.8	Very good
	c	18	96.96	25.8	4	5.7	Good
	d	18	98.62	18.0	5	8.4	Excellent
	e	18	98.73	17.2	3	8.8	Excellent

Such as described in the methodology and according to the objectives, to assess the in-site variability of UB1, twenty complexity one model applications were made; the average slope of the predicted versus measured values was of 0.97, ranging between 0.81 and 1.09; the R^2 ranged between 78.09 and 97.76%, with an average of 91.69%; three presented more than 50% of outliers (11 of 18 samples), all others presented less than 33% (less than 6 outliers of 18 samples); the RMSEP ranged between 22 and 84°C, with an average of 48°C; and the RPD values ranged from 1.7 to 5.2 (Table 11).

According to the RPD classification, the accuracy of the MTR predictions was very poor in four model applications, poor in three, good in two, very good in one, and fair in the other ten. According to the hypothesis, and considering that most models could at least fairly predict the MTR, the in-site variability of site UB1 seems to be low, which suggests that site UB1 has considerable homogenous soil characteristics. Moreover, theoretically it would be expected that models of neighbor sampling points would more accurately predict each other, however this was not empirically true; examples are in using model 'b' to predict the set of samples from sampling point *a*, or using model *b* to predict the set of samples of sampling point *c*, and others that can be seen in Table 11.

Table 11 Results of the application of complexity one models (MC1), for site UB1.

Sampling point code	Applied model code	Slope	R ² %	Outliers number	RMSEP °C	RPD	Class
a	b	0.84	86.06	11	80	1.9	Very poor
	c	1.01	92.36	3	42	3.5	Fair
	d	1.02	95.97	2	31	4.9	Fair
	e	0.96	96.84	2	29	5.2	Good
b	a	0.99	93.15	2	38	4.0	Fair
	c	1.02	95.42	3	31	4.7	Fair
	d	1.01	97.76	2	22	7.0	Very good
	f	0.95	93.59	4	40	3.6	Fair
c	a	0.94	92.35	4	45	3.4	Fair
	b	0.81	89.85	5	84	1.7	Very poor
	d	0.93	92.58	1	47	3.2	Fair
	f	0.90	90.16	1	58	2.5	Poor
d	a	1.06	94.84	3	39	3.9	Fair
	b	0.89	87.79	11	66	2.1	Very poor
	c	0.98	92.50	11	43	3.4	Fair
	e	0.94	95.74	3	37	4.1	Fair
e	a	1.09	78.09	3	76	2.0	Very poor
	b	0.99	87.05	4	55	2.6	Poor
	c	1.00	84.90	6	59	2.5	Poor
	d	1.04	96.79	3	30	5.1	Good

2. To assess the accuracy of the maximum temperatures reached (MTR) predictions using models with increasing complexity twenty five models were constructed; models complexity 2 (MC2), three (MC3), and four (MC4). These models are described in Table 10. The R² of these models ranged from 95.5 to 98.20%, the RMSECV ranged from 20.3 to 32.1°C, and the ranks of the PLS regression ranged from 3 to 5. The RPD of the models ranged from 4.7 to 7.5, thus considered fair to very good models (Table 12).

Table 12 Calibration parameters of models complexity two (MC2), three (MC3), and four (MC4), of site UB1. *n*= number of samples (spectra + MTR in the oven) in the data set

Site code	MC level	Model code	Data n	R ² %	RMSECV °C	Rank	RPD	Class
UB1	MC2	a & b	36	97.29	24.3	5	6.2	Very good
		a & c	36	96.41	28.9	5	5.3	Good
		a & d	36	96.98	26.9	4	5.7	Good
		a & e	36	98.22	20.3	4	7.5	Very good
		b & c	36	97.31	24.4	4	5.9	Good
		b & d	36	96.86	26.3	3	5.7	Good
		b & e	36	96.98	25.8	4	5.8	Good
		c & d	36	95.96	30.8	5	5.0	Good
		c & e	36	95.45	32.1	3	4.7	Fair
		d & e	36	97.93	22.0	5	7.0	Very good
	MC3	a & b & c	54	97.16	25.0	5	6.0	Good
		a & b & d	54	97.23	24.9	5	6.1	Good
		a & b & e	54	97.43	23.9	5	6.3	Good
		a & c & d	54	97.11	25.7	5	5.9	Good
		a & c & e	54	95.79	30.9	3	4.8	Fair
		a & d & e	54	97.58	23.7	5	6.5	Very good
		b & c & d	54	97.25	24.6	3	6.1	Good
		b & c & e	54	96.45	27.9	3	5.4	Good
		b & d & e	54	96.61	27.9	4	5.5	Good
		c & d & e	54	95.97	30.4	4	5.0	Good
	MC4	a & b & c & d	72	96.89	26.3	5	5.7	Good
		a & b & c & e	72	96.20	29.1	3	5.2	Good
		a & b & d & e	72	97.40	24.2	5	6.3	Good
		a & c & d & e	72	95.99	30.3	4	5.0	Good
		b & c & d & e	72	96.34	28.6	4	5.3	Good

Still concerning the calibrations of the models, it would be expected that the more data used in the calibrations the better the validation parameters, however this improvement was not verified. In fact, it was possible to obtain three excellent validations using models *d*, *e*, and *j*, however with MC2, MC3 and MC4 non excellent validation was achieved.

The 25 models presented in Table 12 were applied to the set of samples not included in its calibration. In total, 55 model applications were made.

The slope of true versus predicted values of models complexity two (MC2) ranged between 0.91 and 1.07, with an average of 0.98, for models complexity three (MC3) it

ranged between 0.89 and 1.06, with the average of 0.99, and for models complexity four (MC4) it ranged between 0.92 and 1.04, with the same average of MC3, of 0.99 (Table 13). Compared to the results of the application of MC1 models the minimum and the average values of the slope of the predicted versus measured values were always higher for all types of models, and the maximum values were always lower, which indicates a better accuracy of these models in terms of this parameter.

The R^2 ranged: from 86.57 to 99.07% for MC2; from 88.75 to 97.12% for MC3; and from 83.51 to 97.25% for MC4. The averages of the R^2 were 93.51, 94.23, and 93.43% for MC2, MC3, and MC4, respectively (Table 13). Compared to the applications of MC1 models, the R^2 also indicates a slightly better fit of the true versus predicted values since the average of MC1 model applications was of 91.69%, also lower than in any of these set of models.

Table 13 Results of the slope of true versus predicted values, and of the R^2 (in %) from the application of models complexity two (MC2), three (MC3) and four (MC4) of site UB1.

MC level	MC2 (30 models)		MC3 (20 models)		MC4 (5 models)	
Parameter	Slope	R^2	Slope	R^2	Slope	R^2
Min	0.91	86.57	0.89	88.75	0.92	83.51
Max	1.07	99.07	1.06	97.12	1.04	97.25
Average	0.98	93.51	0.99	94.23	0.99	93.43

Because the interest of this part of the study is to assess whether the enrichment of data is positive or negative to the predictions accuracy, the presentation of results was simplified by using the averages (when applicable) of the RMSEP, the number of outliers, and the RPD, separating them by sampling point and model complexity.

The RMSEP did not vary much among sampling point and model complexity; for complexity one models (MC1) the RMSEP ranged from 33 ± 8 to $58 \pm 18^\circ\text{C}$, for complexity two models (MC2) from 34 ± 6 to $45 \pm 12^\circ\text{C}$, and for complexity three models (MC3) from 29 ± 6 to $48 \pm 13^\circ\text{C}$, and for complexity four models (MC4) the RMSEP

ranged from 24 to 54°C (Table 14). However, predictions accuracy suffered in most cases a slight increase with the increase in model complexity, with the exception of sampling point "b" from MC1 to MC2, and of "c" and "e" from MC2 to MC3 (Table 14).

Table 14 Results of the average RMSEP (in °C) of the MTR predictions plus its standard deviation (when applicable), using models of site UB1. MC= model complexity; n°= number of model applications

MC level	Models n°	Sampling point set of samples				
		a	b	c	d	e
1	4	46 ± 24	33 ± 8	58 ± 18	46 ± 14	55 ± 19
2	6	34 ± 6	35 ± 10	45 ± 12	42 ± 11	44 ± 12
3	4	32 ± 3	29 ± 6	48 ± 13	35 ± 3	46 ± 7
4	1	32	24	47	26	54

Concerning the number of outliers, the number of outliers ranged from: 3 ± 1 to 7 ± 5 for MC1; from 1 ± 1 to 8 ± 4 for MC2; from 1 ± 1 to 8 ± 3 for MC3; and from 0 to 7 for MC4. A decrease in the number of outliers with the increase of model complexity was identified in a, b and c, but not in d, and e, and most model applications presented less than 50% of outliers in the predictions (Table 15).

Table 15 Results of the average number of outliers (maximum=18) plus its standard deviation (when applicable), of the MTR predictions using UB1 models. MC= model complexity; n°= number of model applications

MC level	Models n°	Sampling points				
		a	b	c	d	e
1	4	5 ± 4	3 ± 1	3 ± 2	7 ± 5	4 ± 1
2	6	1 ± 1	2 ± 1	1 ± 1	8 ± 4	6 ± 3
3	4	2 ± 1	1 ± 1	1 ± 3	8 ± 3	5 ± 7
4	1	1	0	1	7	5

The RPD of the MTR predictions using models based on the samples from site UB1 ranged: from 2.7 ± 0.8 to 4.8 ± 1.5 for MC1; from 3.6 ± 1.1 to 4.8 ± 1.5 for MC2; from 3.3 ± 0.5 to 5.4 ± 0.9 for MC 3; and from 3.2 to 6.4 for MC4 (Table 16). The hypothesis that the increase in model complexity would imply an improvement in models accuracy was only verified in *a*, *b*, and *d*, moreover this improvement was not linear. The results are quite diverse among sampling points; for example results show that for sampling point *b* the variability contained in complexity one (MC1) is already enough for a good prediction, however for sampling point *c* not even complexity four model (MC4) gave such an accurate prediction as the one mentioned before.

Table 16 Results of the average RPD plus its standard deviation (when applicable), of the MTR predictions using UB1 models. MC= model complexity; n^o= number of model applications

MC	Models	Sampling points				
level	n ^o	a	b	c	d	e
1	4	3.9 ± 1.5	4.8 ± 1.5	2.7 ± 0.8	3.4 ± 0.9	3.0 ± 1.4
2	6	4.6 ± 0.9	4.8 ± 1.5	3.6 ± 1.1	3.8 ± 1.0	3.7 ± 1.2
3	4	4.7 ± 0.3	5.4 ± 0.9	3.3 ± 0.9	4.6 ± 1.0	3.3 ± 0.5
4	1	4.7	6.4	3.2	5.9	2.8

Site UB2

1. To assess the NIR-identified soil variability of site UB2, models complexity one (MC1) were constructed using the set of samples of each sampling point of UB2. Concerning the validation of these models, the values of the R^2 ranged from 95.18 to 98.53%, the RMSECV ranged from 17.4 to 32.1°C, the ranks of the PLS regressions ranged from 3 to 5, and the RPD values ranged from 4.5 to 8.1 (Table 17). The number of outliers of the models ranged from 0 to 2 (not removed). Based on the RPD classification, these models have fair to excellent prediction capability.

Table 17 Calibration parameters of complexity one models (**MC1**), of site UB2. *n*= number of samples (spectra + MTR in the oven) in the data set.

Site code	Model code	Data n	R ² %	RMSECV °C	Rank	RPD	Class
UB2	f	19	95.18	32.1	3	4.5	Fair
	g	18	96.61	27.2	5	5.4	Good
	h	18	98.28	20.4	4	7.6	Very good
	i	18	97.48	23.8	5	6.2	Very good
	j	18	98.53	17.4	4	8.1	Excellent

In terms of the accuracy of predictions, the model applications of site UB2 were very different from the ones from UB1. The average slope of the predicted versus measured values was of 0.83, ranging from 0.10 to 1.09; the R² ranged from negative values to 94.58%, with an average of 74.44%; the RMSEP ranged from 40 to 563°C, from which ten out of 20 were higher than 100°C; the number of outliers was maximum in ten out of 20 model applications, nevertheless the other ten had less than 50% of outliers in the prediction sets (Table 18). Compared to the results of UB1 the accuracy of predictions of UB2 was quite low. According to the hypothesis, and because the models result in poor predictions these results suggest that the in-site variability of UB2 was high, and the site is quite heterogeneous in terms of soil characteristics.

Table 18 Results of the application of complexity one models (MC1), of site UB2.

Sampling point code	Applied model code	Slope	R ² %	Outliers number	RMSEP °C	RPD	Class
f	g	1.05	85.25	3	58	2.5	Poor
	h	0.71	53.06	19	150	1.0	Very poor
	i	0.88	89.66	2	63	2.4	Poor
	j	0.85	73.77	8	90	1.6	Very poor
g	f	0.96	89.27	2	50	2.9	Poor
	h	0.67	33.96	18	181	0.9	Very poor
	i	0.92	87.37	2	59	2.5	Poor
	j	0.88	89.58	3	63	2.2	Very poor
h	f	0.10	*	17	563	0.3	Very poor
	g	0.69	*	18	267	0.5	Very poor
	i	0.87	94.58	12	60	2.5	Poor
	j	0.80	*	18	187	0.8	Very poor
i	f	0.86	*	18	201	0.7	Very poor
	g	0.87	*	18	217	0.7	Very poor
	h	0.92	86.03	2	62	2.5	Poor
	j	0.88	52.61	18	110	1.3	Very poor
j	f	1.09	*	18	158	0.9	Very poor
	g	0.93	94.38	18	40	3.6	Fair
	h	0.65	23.96	18	191	0.8	Very poor
	i	1.01	88.63	8	49	3.0	Poor

**negative results

2. To assess the accuracy of the MTR predictions using with increscent model complexity, models with successive increase in data were constructed (MC2, MC3, and MC4). Concerning the calibration parameters of all models, the values of the R² ranged from 92.12 to 97.67%, the RMSECV ranged from 23.4 to 41.9°C, the ranks of the PLS regression ranged between 4 and 5. The RPD values ranged from 3.6 to 6.6, slightly lower values compared to site UB1 that ranged from 4.7 to 7.5. Nevertheless, these models have fair to very good prediction capability (Table 19).

Table 19 Calibration parameters of models complexity two (MC2), three (MC3), and four (MC4) of site UB2. *n*= number of samples (spectra + MTR in the oven) in the data set

Site code	MC level	Sampling points code	Data n	R ² %	RMSECV °C	Rank	RPD	Class
	MC2	f & g	37	96.88	26.0	5	5.7	Good
		f & h	37	96.70	27.4	5	5.6	Good
		f & g	37	96.35	28.3	5	5.3	Good
		f & j	37	96.61	27.2	5	5.4	Good
		g & h	36	95.27	33.0	4	4.7	Fair
		g & i	36	96.36	28.4	5	5.3	Good
		g & j	36	97.10	24.8	4	6.0	Good
		g & h	36	97.67	23.4	5	6.6	Very good
		g & i	36	96.84	26.7	5	5.7	Good
		i & j	36	96.87	26.0	5	5.7	Good
UB1	MC3	f & g & h	55	96.04	29.9	5	5.1	Good
		f & g & i	55	96.48	27.8	5	5.4	Good
		g & g & j	54	96.81	26.1	5	5.6	Good
		f & h & i	55	96.97	26.2	5	5.7	Good
		f & h & j	55	93.31	38.5	5	3.9	Fair
		f & i & j	55	95.60	30.8	5	4.8	Fair
		g & h & i	54	96.51	28.3	5	5.4	Good
		g & h & j	54	92.12	41.9	5	3.6	Fair
		g & i & j	54	96.08	29.2	5	5.1	Good
		h & i & j	54	96.87	26.5	5	5.7	Good
	MC4	f & g & h & i	73	96.47	28.2	5	5.4	Good
		f & g & h & j	73	93.38	38.2	5	3.9	Fair
		f & g & i & j	73	96.07	29.2	5	5.1	Good
		f & h & i & j	73	94.79	34.0	5	4.4	Fair
		g & h & i & j	72	93.19	39.0	5	3.9	Fair

Such as in the case of site UB1, also in UB2 fifty five model applications were made.

The slope of true versus predicted values of models complexity two (MC2) ranged between 0.29 and 1.28, with an average of 0.94, for models complexity three (MC3) it ranged between 0.79 and 1.30, with the average of 0.99, and for models complexity four (MC4) it ranged between 0.79 and 1.26, with the average of 0.98 (Table 20) Which

indicates a improvement of results especially from MC2 to MC3, and also compared to the results of the application of MC1 that resulted in an average of only 0.83 (see Table 18)

The R^2 ranged: from a negative value to 96.61% for MC2; from 17.00 to 98.34% for MC3; and from 34.84 to 93.63% for MC4. The averages of the R^2 were 56.99, 78.03, and 74.41% for MC2, MC3, and MC4, respectively (Table 20). Such as in the case of the previous parameter the R^2 also indicates a marked improvement of the average results from MC2 to MC3. The values of the R^2 from the application of MC1 (that ranged from negative values to 94.58%, with an average of 74.44%) are similar to the results of MC4, however. in MC4 no negative values were obtained, which indicates that the increase in model complexity was positive.

Table 20 Results of the slope of true versus predicted values, and of the R^2 (in %) from the application of models complexity two (MC2), three (MC3) and four (MC4) of site UB2.

MC level	MC2 (30 models)		MC3 (20 models)		MC4 (5 models)	
Parameter	Slope	R^2	Slope	R^2	Slope	R^2
Minimum	0.29	*	0.79	17.00	0.79	34.84
Maximum	1.28	96.61	1.30	98.34	1.26	93.63
Average	0.94	56.99	0.99	78.03	0.98	74.41

*negative value

Such as in the case of the within-site analysis in site UB1, the presentation of results of the next parameters (RMSEP, number of outliers and RPD) was simplified by using the averages (when applicable) of the calculated parameters separating them by sampling point and model complexity.

The precision of the MTR predictions using models from UB2 was quite variable between sampling points; for MC1 the RMSEP ranged from 88 ± 62 to $269 \pm 214^\circ\text{C}$; for MC2 it ranged from 49 ± 14 to $186 \pm 142^\circ\text{C}$, for MC3 from 43 ± 15 to $119 \pm 32^\circ\text{C}$, and for MC4 from 39 to 125°C (Table 21). In terms of the RMSEP, the accuracy of the predictions increased with the increase of models complexity with the exception of sampling point j. These results suggest that the variability introduced by the set of samples from more

sampling points improve the predictions, however for two sampling points this variability doesn't seem to be enough.

Table 21 Results of the average RMSEP (in °C) of the MTR predictions plus its standard deviation (when applicable), using models of site UB2. MC= model complexity; n°= number of model applications

MC level	Models n°	Sampling points				
		f	g	h	i	j
1	4	90 ± 42	88 ± 62	269 ± 214	148 ± 74	109 ± 76
2	6	51 ± 15	49 ± 14	186 ± 142	91 ± 92	90 ± 27
3	4	45 ± 17	48 ± 15	119 ± 32	43 ± 15	97 ± 54
4	1	45	50	124	39	125

The number of outliers of the MTR predictions decreased with the increase in model complexity, however this decrease was not linear and more pronounced in the sampling point set of samples *f*, *g* and *i*, which decreased from 8 ± 8 to 0, 6 ± 8 to 1, and 14 ± 8 to 3, respectively. The predictions of the set of samples from sampling points *h* and *j* resulted in high number of outliers (more than 50%) for all MC levels (Table 22).

Table 22 Results of the average number of outliers (maximum= 18 or 19) plus its standard deviation (when applicable), of the MTR predictions using UB2 models. MC= model complexity; n°= number of model applications

MC level	Models n°	Sampling point set of samples				
		f	g	h	i	j
1	4	8 ± 8	6 ± 8	16 ± 3	14 ± 8	16 ± 5
2	6	4 ± 7	4 ± 7	14 ± 4	9 ± 9	14 ± 6
3	4	1 ± 1	1 ± 1	14 ± 3	5 ± 7	10 ± 10
4	1	0	1	13	3	12

The RPD of the MTR predictions using models based on the samples from site UB2 ranged: from 1.0 ± 1.3 to 2.1 ± 1.5 for MC1; from 1.7 ± 0.9 to 3.4 ± 1.0 for MC2; from 1.4 ± 0.5 to 3.8 ± 1.0 for MC 3; and from 1.2 to 3.9 for MC4 (Table 23). Using the RPD as assessment tool, the hypothesis that the increase in model complexity would imply an improvement in models accuracy was only verified in the predictions of the set of samples of sampling point *i*, and this improvement was not linear. Such as in site UB1 the results are quite diverse among sampling points; however the accuracy of predictions is smaller in all cases. Results show that when the variability of samples *h* and *j* are not included in the models the MTR of these samples can't be predicted.

Table 23 Results of the average RPD plus its standard deviation (when applicable), of the MTR predictions using UB2 models. MC= model complexity; n° = number of model applications

MC	Models	Sampling points				
level	n°	f	g	h	i	j
1	4	1.9 ± 0.7	2.1 ± 0.9	1.0 ± 1.3	1.3 ± 0.8	2.1 ± 1.5
2	6	3.2 ± 0.9	3.4 ± 1.0	1.7 ± 0.9	2.7 ± 1.4	1.8 ± 0.5
3	4	3.7 ± 1.1	3.4 ± 1.0	1.4 ± 0.5	3.8 ± 1.0	2.8 ± 3.0
4	1	3.4	3.0	1.2	3.9	1.2

2.3.1.2 Between-site analysis

1. In this part of the study, first a model constructed with all set of samples from UB1 was used to predict the maximum temperatures reached by samples from UB2, and a model constructed with all set of samples from UB2 was used to predict the set of samples of UB1. The validation of model UB1 achieved good calibration parameters with RMSECV of 29.1°C, R^2 of 96.24%, rank 4, and RPD of 5.2. Model UB2 was classified as a fair calibration with RMSECV of 38.5°C, r^2 of 93.3°C, rank 5, and RPD of 3.9 (Table 24).

Table 24 Calibration parameters of models UB1, and UB2. n = number of samples (spectra + MTR in the oven) in the data set

Model code	Sampling points codes	Data n	R ² %	RMSECV °C	Rank	RPD	Class
UB1	a & b & c & d & e	90	96.24	29.1	4	5.2	Good
UB2	f & g & h & i & j	91	93.3	38.5	5	3.9	Fair

The MTR predictions from the application of model UB2 to the sampling points of site UB1 were quite accurate. The average slope of the predicted versus measured values ranged from 0.93 to 1.00; the R² ranged from 92.33 to 96.23%, the values of the RMSEP ranged from 30 to 46°C, the number of outliers ranged from 0 to 2, the RPD values ranged from 3.1 to 5.0, thus considered fair to good predictions. The predictions using model UB1 applied to UB2 samples were not as accurate as the previous ones. The average slope ranged from 0.83 to 1.20; the R² ranged from 60.03 to 96.36%, the values of the RMSEP ranged from 32 to 115°C, and the number of outliers ranged from 2 to 16, the RPD indicated two very poor, and three fair predictions (Table 25).

Table 25 Results of the application of models UB1 and UB2 to the samples of UB2 and UB1, respectively.

Model code	Applied to sampling point	Slope	R ² %	Outliers n ^o	RMSEP °C	RPD	Class
UB2	a	0.98	95.30	1	33	4.6	Fair
	b	0.93	92.33	2	46	3.1	Fair
	c	0.94	92.43	0	45	3.2	Fair
	d	0.93	95.42	1	41	3.7	Fair
	e	1.00	96.23	0	30	5.0	Good
UB1	f	1.01	94.50	2	35	4.1	Fair
	g	1.05	96.36	2	32	4.6	Fair
	h	0.83	60.03	16	115	1.3	Very poor
	i	1.07	94.55	8	41	3.6	Fair
	j	1.20	92.96	15	63	2.2	Very poor

2. Successful calibrations were obtained using the samples from two-site models or complexity nine models (MC9). The R^2 ranged from 93.09 to 96.19%, the RMSECV ranged from 29 to 39°C, the ranks ranged between 4 and 5, and the RPD values ranged from 3.8 to 5.2, resulting in fair to good models (Table 26).

Table 26 Calibration parameters of the two-site or complexity nine models (MC9). n = number of samples (spectra + MTR in the oven) used in the data set

Model code	Sampling points codes	Data n	R^2 %	RMSECV °C	Rank	RPD	Class
All - a	UB1 (b & c & d & e) & UB2 (f & g & h & i & j)	162	93.72	37	5	4.0	Fair
All - b	UB1 (a & c & d & e) & UB2 (f & g & h & i & j)	162	93.87	37	4	4.1	Fair
All - c	UB1 (a & b & d & e) & UB2 (f & g & h & i & j)	162	94.81	34	5	4.4	Fair
All - d	UB1 (a & b & c & e) & UB2 (f & g & h & i & j)	162	93.09	39	4	3.8	Fair
All - e	UB1 (a & b & c & d) & UB2 (f & g & h & i & j)	162	93.55	38	4	4.0	Fair
All - f	UB1 (a & b & c & d & e) & UB2 (g & h & i & j)	163	93.68	38	4	4.0	Fair
All - g	UB1 (a & b & c & d & e) & UB2 (f & h & i & j)	162	93.73	38	5	4.0	Fair
All - h	UB1 (a & b & c & d & e) & UB2 (f & g & i & j)	162	96.19	29	5	5.2	Good
All - i	UB1 (a & b & c & d & e) & UB2 (f & g & h & j)	162	94.50	35	4	4.3	Fair
All - j	UB1 (a & b & c & d & e) & UB2 (f & g & h & i)	162	93.69	38	4	4.0	Fair

Concerning the applications of complexity nine models (MC9), the application of model All-h to the set of samples of h resulted in a very poor prediction with RPD of 1.1, slope of true versus predicted samples of 0.77, r^2 of 53.55%, twelve outliers, and RMSEP of 138°C. The other nine model applications resulted in acceptable predictions (poor to very good) with the RPD ranging from 2.6 to 7.5, the slope of true versus predicted values ranged from 0.92 to 1.17, the R^2 ranged from 89.78 to 98.27%, and the values of the RMSEP ranged from 20 to 55°C, and the number of outliers ranged from zero to two (Table 27).

Once again, results suggest that sampling point h seems to differ significantly from the others, however when it is included in models for the MTR prediction of other samples, it

doesn't seem to "harm" the results, and moreover in some cases even improve the predictions. This suggests that the variability introduced by these samples in the models is positive for the predictions. However, for sampling point j a marked improvement of the predictions was obtained; obtaining only one outlier using the model All-j, which is another indicator that the increase of model complexity is positive for the prediction accuracy.

Table 27 Results of the application of the two-site or complexity nine models (MC9).

Model code	Applied to code	Slope	R ² %	Outliers n ^o	RMSEP °C	RPD	Class
All - a	a	1.00	96.37	0	29	5.2	Good
All - b	b	0.96	95.28	0	33	4.5	Fair
All - c	c	0.92	89.78	0	55	2.7	Poor
All - d	d	1.00	98.27	0	20	7.4	Very good
All - e	e	1.03	96.90	1	28	5.3	Good
All - f	f	0.96	94.01	0	38	4.0	Fair
All - g	g	0.96	91.79	0	44	3.4	Fair
All - h	h	0.77	53.55	12	138	1.1	Very poor
All - i	i	1.07	90.69	2	50	3.0	Poor
All - j	j	1.17	95.97	1	51	2.9	Poor

Concerning all models constructed in this section of this paper, similar (leave-one-out cross)-validations of NIR-based models for the prediction of soil maximum temperatures reached (MTR) were found in the literature. In Guerrero et al. (2007) study, validation parameters of NIR-based local models for MTR prediction presented values of R² that ranged from 97.47 to 98.56%, RMSECV that ranged from 25.0 to 32.5°C, and RPD values always higher than 6.2, however with higher ranks that ranged from 7 to 9. In Arcenegui et al. (2008) study the best model had R² of 98.70%, RMSECV of 23.6°C, rank 8, and RPD of 8. Moreover, in Arcenegui et al., (2010) the best models had RMSECV ranging from 21.8 to 28.2°C, R² from 98.20 to 99.00%, RPD higher than 6.5, and ranks ranging from 3 to 8. In these three studies, 60 to 70 data samples were used in the model validations. Moreover, in Maia et al., (2012) study the NIR-based model used for the MTR estimation of wildfire-burnt soil samples had R² and RMSECV of 97.0% and 35.0°C, respectively,

and used three PLS vectors (rank). Worth stressing that in these four studies the collected forest soil samples were mixed to perform a composite sample, and in this study the forest samples were maintained separately so that individual models from each sampling points were obtained. The present work didn't include the differences between using composite or separate field samples as research question, thus no composite sample was made, however strongly recommended in future studies.

In Lugassi et al. (2010) study, the best achieved models had poorer validation parameters (RMSECV of 17°C and 15°C; R^2 of 93% and 95%; ranks 5 and 4, and RPD of 3.9 and 4.4, respectively) than in most models of this study, nevertheless concerning the application of models to samples of known MTR (measured during a controlled fire) good predictions were obtained, with RPD's of 5 and 4.

Concerning the evolution of the response of all models build in this sub-chapter and using as assessment tool the RPD of all model applications represented in Figure 2, it is easily seen that the RPD values were not always higher for models with the increase in model complexity (more data from other sampling points) as it was hypothesized: in sampling points *a*, *c*, and *h* the increase of model complexity had a very slight effect in the RPD value with the increase in model complexity (from MC1 to MC9); in sampling point *b* and *d* the RPD increased from MC1 to MC4, decreased from MC4 to UB2, and increased again from UB2 to MC9. However, in sampling points *e*, *f*, *g*, *j*, and *i* the general tendency, although irregular was for an increase of the RPD from MC1 to MC9 (Figure 2).

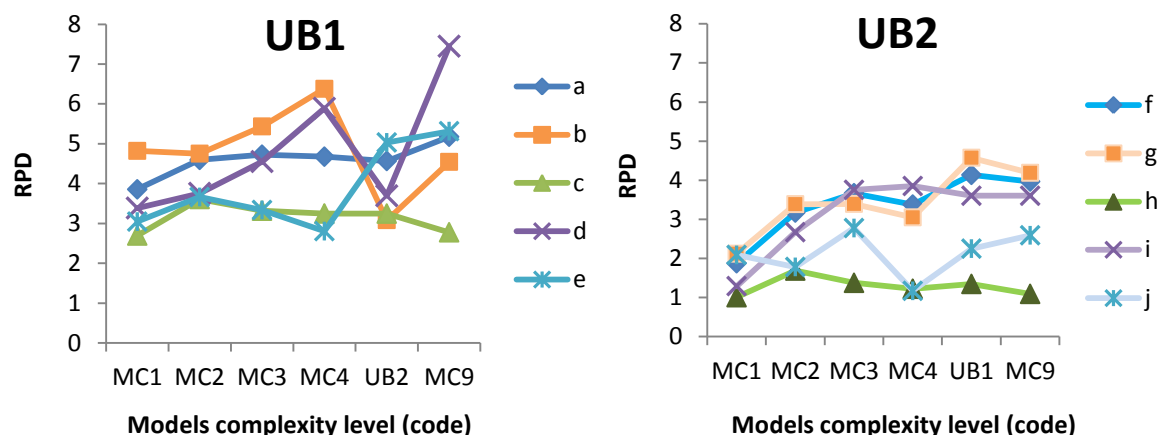


Figure 2 Results of the RPD of all model applications, organized by the type of models applied to the ten sampling points of each site. The lines don't indicate continuity of data, but were maintained to facilitate the observation of results.

One of the key aspects of this technique must be the representativeness of the calibration or model. The model must contain the variability contained in the samples for prediction. This variability is determined by the natural variation that exists in the soil of the study area and that is exerted by the forest fire. Thus, the calibration should contain all sources of variation that are found in the estimated samples. If only the variability induced by heat is considered, the model must contain spectra of samples burned at different temperatures and different times. Considering the fire variability, and the fact that the samples may contain ash, this variable must also be included during calibration. Similarly, soil characteristics have a spatial variation, which should also be integrated into the calibration. All factors that influence the spectra should be integrated in the calibrations. In this study, all soil samples were treated in a way that the variability of the samples for prediction was only influenced by the natural soil variation and the maximum temperatures reached. Even though the high variety of responses of the models constructed in this sub-chapter, indicates that obtaining a robust calibration is not an easy task. Nevertheless, considering the simplicity and speed of the work, the inclusion of these factors in the calibration can be achieved with moderate effort, and the results of its application can be used as screening for soil burn severity classifications.

2.3.2 MODEL ASSESSMENT BASED ON WILDFIRE-BURNT SOILS

As described in the methodology, in this part of the study two strategies were used in the construction of models for the estimation of the maximum temperatures reached (MTR) of the wildfire-burnt samples. Results of the both strategies are presented next.

2.3.2.1 Strategy 1 (S1)

Three models, namely UB1', UB2', and (UB1+UB2)' were successfully calibrated and validated for MTR estimations of the wildfire-burnt samples. The slope of the true versus predicted samples was approximately 1.0 in the three models, the values of the R^2 were 96.24, 96.90, and 96.10%, the RMSECV were 29.1, 26.2, and 29.5°C, and the RPD values were 5.2, 5.8, and 5.1, respectively in UB1', UB2', and (UB1+UB2)'. According to the RPD classification used, these are considered good models. For some authors RPD values higher than 5 can be considered as excellent models (Malley et al., 1999). The ranks of the PLS regression were 4, 8, and 9, and the number of outliers of the calibration set ranged from 0 to 1 (Figure 2).

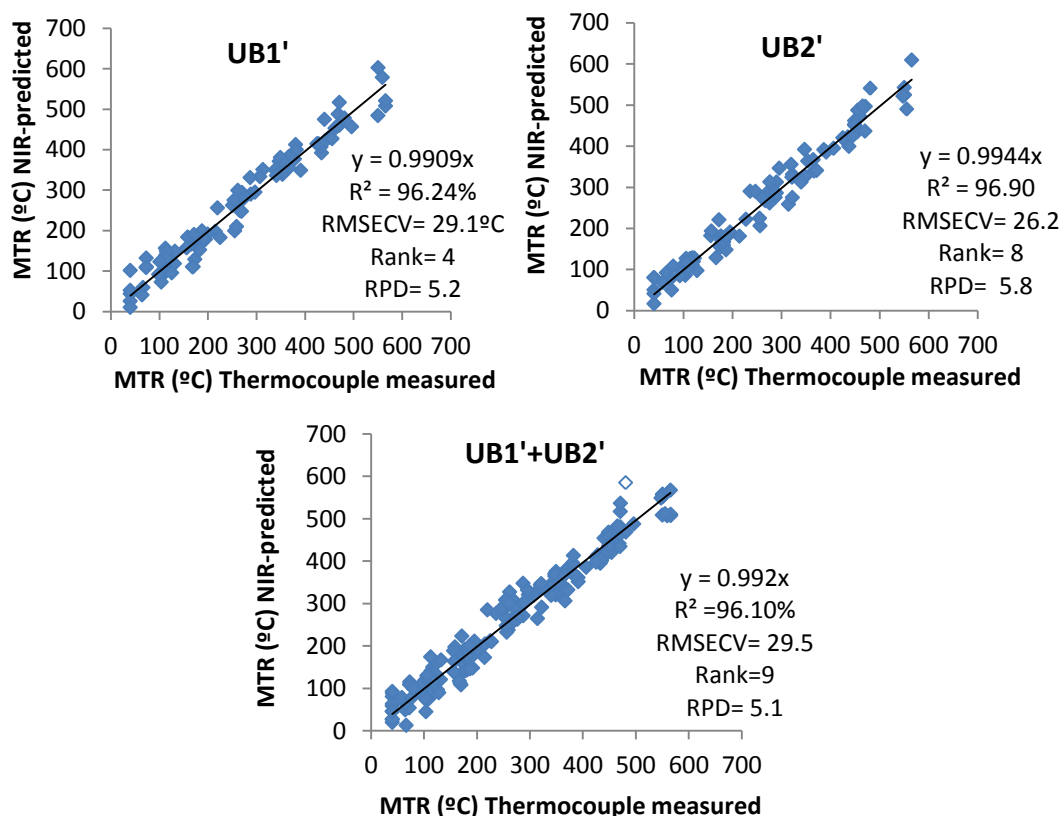


Figure 3 Relation between maximum temperatures reached in the soil samples measured with thermocouple and predicted by near-infrared spectroscopy in the validations of S1 models. Unfiled points denote outliers (not removed).

For site B1, the maximum temperatures reached (MTR) estimations resulted in high number of outliers (80 and 90%) for the three models. Nevertheless, the surface MTR estimations were higher than the underneath MTR estimations (Table 28).

For site B2, all three models discriminated samples by depth, with the exception of samples from sampling point 7, using model UB2. The MTR estimations resulted in 50% of outliers using model UB1', and 45% of outliers using the other two models (Table 29).

For site B3, the MTR estimations resulted in 60, 40, and 50% of outliers, respectively using models UB1', UB2', and UB1+UB2', and all the surface MTR estimations were higher than the underneath MTR estimations (Table 30).

Table 28 Results of the MTR estimations (in °C) of site B1 using S1 models. The asterisk denotes outliers.

Site code	Sampling point code	Sample depth cm	UB1' Rank 4	UB2' Rank 8	UB1+UB2' Rank 9
B1	I	0-2	344*	430*	296*
		2-5	273*	397*	256*
	II	0-2	331*	430*	317*
		2-5	225*	350*	249*
	III	0-2	345*	438*	318*
		2-5	290*	368*	274*
	IV	0-2	135*	301*	269*
		2-5	69	137*	155*
	V	0-2	251*	272	208*
		2-5	149	178	119

Table 29 Results of the MTR estimations (in °C) of site B2 using S1 models. The asterisk denotes outliers.

Site code	Sampling point code	Sample depth cm	UB1' Rank 4	UB2' Rank 8	UB1+UB2' Rank 9
B2	1	0-2	305*	412*	296*
		2-5	131*	213	113
	2	0-2	221*	321*	218*
		2-5	94	167	85
	3	0-2	247*	372*	259*
		2-5	104	184	106
	4	0-2	258*	347	278
		2-5	104	178	120
	5	0-2	132	202	136
		2-5	57	121	44
	6	0-2	351*	437*	335*
		2-5	223*	335*	230*
	7	0-2	116*	216*	250*
		2-5	102	219*	112
	8	0-2	271	387	287*
		2-5	147	242	178
	9	0-2	257*	351*	261*
		2-5	153	236	166
	10	0-2	252*	344	243*
		2-5	114	191*	79

Table 30 Results of the MTR estimations (in °C) of site B3 using S1 models. The asterisk denotes outliers.

Site code	Sampling point code	Sample depth cm	UB1' Rank 4	UB2' Rank 8	UB1+UB2' Rank 9
B3	α	0-2	266*	338	261*
		2-5	190	239	159
	β	0-2	245*	323	233
		2-5	153	218	122
	γ	0-2	210*	212*	203*
		2-5	143*	161*	156*
	δ	0-2	129	176	100
		2-5	128*	150*	89*
	ε	0-2	231*	352*	242*
		2-5	171	266	159

2.3.2.1 Strategy 2 (S2)

The same three models of S1 were successfully 'recalibrated' and validated, decreasing the ranks (number of PLS vectors used in the calibration) from 4, 8, and 9 in S1 to 2, 3 and 2 in S2. The slope of the true versus predicted samples of the new S2 models UB1", UB2", and UB1'+UB2' ranged between 0.97 and 0.98, the R2 ranged from 90.03 to 93.16%, the RMSECV ranged from 39.2 to 47.2°C, and the RPD ranged between 3.2 and 3.8. The number of outliers in the calibration sets ranged from 0 to 3 (Figure 3). Such as expected, the validation parameters suffered a decrease in its quality, caused by the decrease in PLS vectors. Nevertheless, based on the RPD classification, these models are considered fair to be applied to the wildfire-burnt samples.

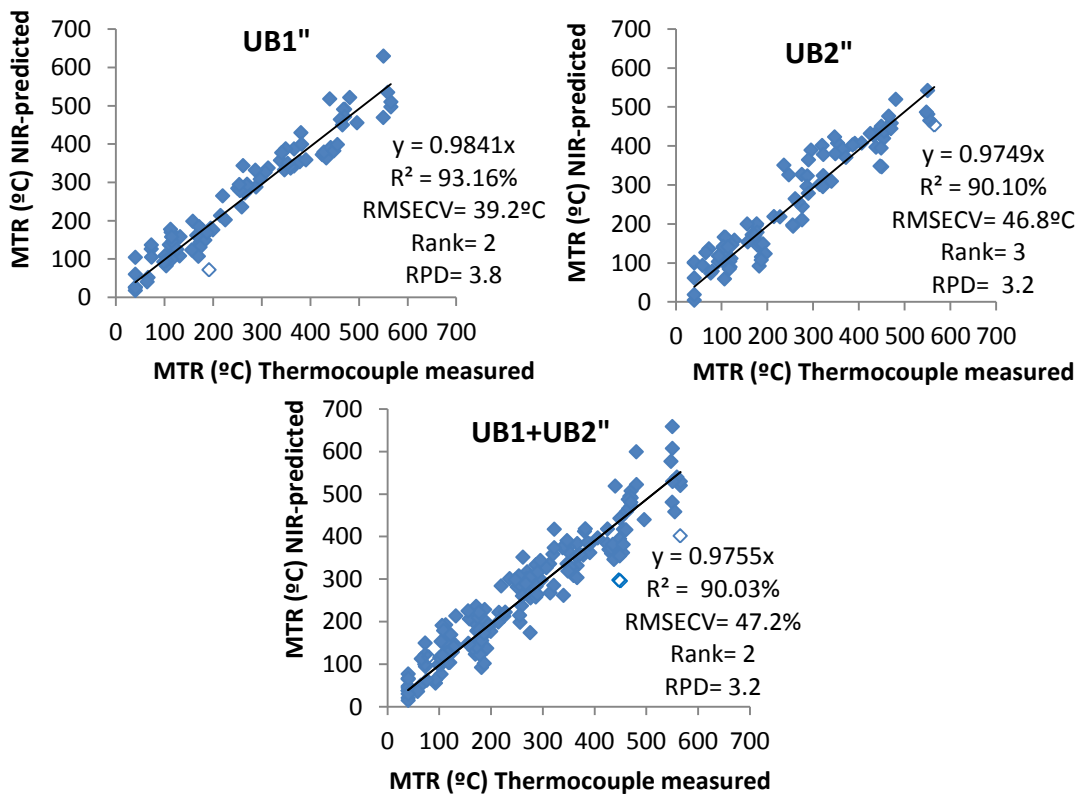


Figure 4 Relation between maximum temperatures reached in the soil samples measured with thermocouple and predicted by near-infrared spectroscopy in the validations of S2 models. Unfiled points denote outliers (not removed).

For site *B1*, the maximum temperatures reached (MTR) estimations resulted in less number of outliers than for the analogous models from Strategy 1 (S1) that had higher ranks, resulting in 10 to 20% of the total number of estimations. The surface MTR estimations were also higher than the underneath MTR estimations (Table 31).

For site *B2*, the MTR estimations also resulted in less number of outliers than for the analogous models from S1, resulting in only one outlier per model application (details of the comparison of results is given more ahead in this paper). Moreover, the models also discriminated samples by depth with the exception of samples from sampling point 7, using models UB1" and UB2" (Table 32).

For *B3* the new strategy of models construction also resulted in a diminishment of the number of outliers in the estimates; resulting in 40% of outliers for model UB1" and UB1+UB2", and 10% in UB2". Also the MTR estimations of the surface samples were higher than of the underneath (Table 33).

Table 31 Results of the MTR estimations (in °C) of site B1 using S2 models. The asterisk denotes outliers.

Site code	Sampling point code	Sample depth cm	UB1" Rank 2	UB2" Rank 3	UB1+UB2" Rank 2
B1	I	0-2	413	418	315
		2-5	346	357	241
	II	0-2	461	414*	334
		2-5	285	313	183
	III	0-2	446	423	317
		2-5	393	375	294
	IV	0-2	258*	228*	168*
		2-5	66	113	80*
	V	0-2	339	349	280
		2-5	206	244	167

Table 32 Results of the MTR estimations (in °C) of site B2 using S2 models. The asterisk denotes outliers.

Site code	Sampling point code	Sample depth cm	UB1"	UB2"	UB1+UB2"
			Rank 2	Rank 3	Rank 2
B2	1	0-2	409	390	315
		2-5	204	212	147
	2	0-2	319	322	229
		2-5	145	167	106
	3	0-2	345	338	256
		2-5	135	170	99
	4	0-2	351	349	273
		2-5	152	188	106
	5	0-2	183	215	140
		2-5	79	129	75
	6	0-2	446	426	343
		2-5	296	314	201
	7	0-2	122*	128*	117*
		2-5	132	174	104
	8	0-2	328	352	241
		2-5	195	221	126
	9	0-2	364	355	260
		2-5	196	224	139
	10	0-2	359	337	258
		2-5	107	147	76

Table 33 Results of the MTR estimations (in °C) of site B3 using S2 models. The asterisk denotes outliers.

Site code	Sampling point code	Sample depth cm	UB1"	UB2"	UB1+UB2"
			Rank 2	Rank 3	Rank 2
B3	α	0-2	344	354	264
		2-5	229	272	177
	β	0-2	341	337	272
		2-5	193	235	144
	γ	0-2	127*	141*	93*
		2-5	78*	108	73*
	δ	0-2	118*	164	72
		2-5	29*	105	47*
	ε	0-2	303	320	196
		2-5	222	260	140

2.3.3 WILDFIRE SOIL MAXIMUM TEMPERATURES REACHED (MTR) ASSESSMENT AND BURN SEVERITY CLASSIFICATION

From strategy one (S1) to strategy two (S2) a diminishment of the amount of outliers was verified (Table 34). This indicated that the hypothesis made that reducing the number of PLS vectors would have a positive impact in the estimates, was correct. However, models from S2 suffered a decrease in quality fit, and the ideal scenario would be to have both, good quality models and low number of outliers.

Table 34 Comparison of the results of the percentage of outliers in the MTR estimations of both strategies (S1 and S2) discriminated by model and site.

Sites	B1		B2		B3	
Model	S1	S2	S1	S2	S1	S2
UB1	80	10	50	5	60	40
UB2	80	20	45	5	40	10
UB1 + UB2	90	20	45	5	50	40

Attending to the amount of outliers, the best model for site B1 would be UB1' of Strategy 2 (S2), for B2 the three models of S2 are of equal quality, and for site B3 the best model would be UB2' also of S2. Considering this, a new criterion for choosing the best MTR estimations was needed, thus an assessment to all MTR estimations was made. This assessment was made by calculating of the standard deviation of results given by all models, and is presented next (estimations considered outliers were also included).

The standard deviation of the MTR estimated by S1 models of the surface samples (0-2 cm depth) varied between 4 and 88°C, with an average of $54 \pm 18^\circ\text{C}$, and in the underneath samples it varied between 9 and 77°C, with an average of $49 \pm 15^\circ\text{C}$, similar results were found in the MTR estimations of the models from strategy two, which standard deviation of surface samples varied between 5 and 69°C, with an average of $48 \pm 15^\circ\text{C}$, and underneath samples between 19 and 68°C, with an average of $43 \pm 13^\circ\text{C}$. The total standard deviation of results ranged from 34 to 64°C, with the average of $49 \pm 9^\circ\text{C}$ (Table 35).

Table 35 Results of the assessment based on the standard deviation of the MTR (in °C) estimated by the three models of S1 and S2 for each depth, and the total standard deviation (six models and both sample depths).

Strategies	S1		S2		Total
	0-2	2-5	0-2	2-5	Both depths
Min (°C)	4	9	5	19	34
Max (°C)	88	77	69	68	64
Average (°C)	54 ± 18	49 ± 15	48 ± 15	43 ± 13	49 ± 9

These results show that the difference between the MTR estimated by the six models was not very high (less than 100°C), however outliers are not considered to be trust worthy. Thus, the criterion used for choosing the best MTR estimations was to exclude models that present more than 50% of outliers. According to this, and looking back to Table 29, for site B1 three models were considered acceptable model, for site B2 five models were considered acceptable models, and for site B3 four models were considered acceptable models. However, even being considering acceptable models, the MTR estimations that appeared as outliers in these models were excluded for presentation.

The MTR estimations of three surface (0-2 cm depth) soil samples (B1-IV, B2-7, and B3-γ) appeared as outliers in all models, suggesting that they have particular proprieties that couldn't be explained by any of the models. In these cases, the selected estimations were the ones that presented the lowest *Mahalanobis* distance. This also suggests that not all the soil variability of the study sites was included in the models. Having this, the results of the MTR estimations of the selected models is presented next.

The estimated maximum temperatures reached (MTR) of site B1 ranged from 228 to 403°C in surface samples (0-2 cm depth), and from 89 to 354°C in underneath samples (2-5 cm depth) (Figure 5).

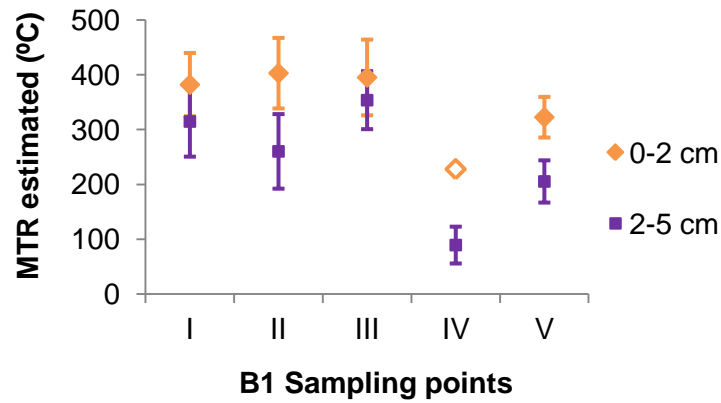


Figure 5 Results of the MTR estimations of site B1 including the standard deviation when more than one model was used for estimation. The unfilled sample was outlier in all MTR estimations.

For site B2 the MTR estimations ranged from 128 to 405°C in surface, and from 90 to 270°C in underneath samples (Figure 6).

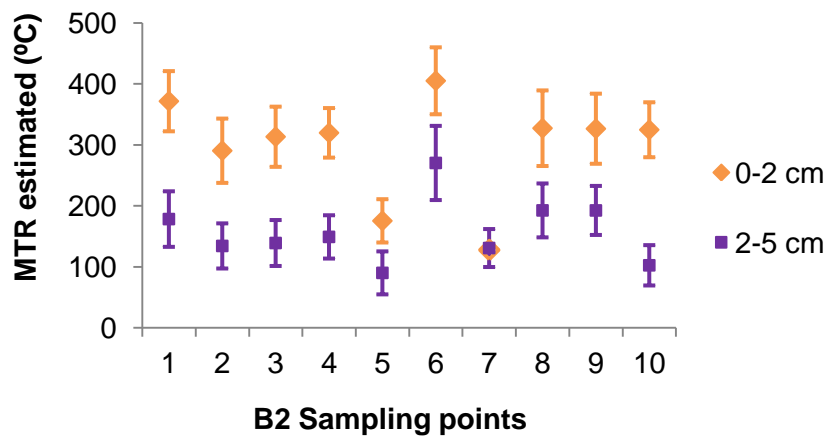


Figure 6 Results of the MTR estimations of site B2 including the standard deviation when more than one model was used for estimation. The unfilled sample was outlier in all estimations (sampling point 7 0-2 cm).

For site B3 the MTR estimations ranged from 138 to 325°C and from 105 to 229°C for 0-2 and 2-5 cm depth samples, respectively (Figure 7).

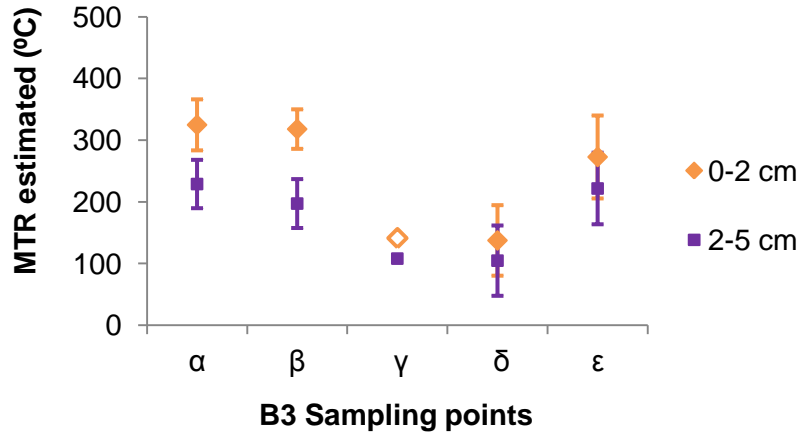


Figure 7 Results of the MTR estimations of B3 including the standard deviation when more than one model was used for estimation. The unfilled sample was outlier in all estimations.

According to the burn severity index proposed in Table 9 of the materials and methods sub-chapter, and considering the surface samples, the soil burn severity in site B1 and B2 was moderate to high, and in B3 was moderate (Table 36). In most cases underneath samples suffered a decrease of one or two levels of burn severity, with the exception of samples III and ϵ that have maintained in the same burn severity level.

Table 36 Classification of the soil burn severity of both surface (0-2 cm depth) and underneath (2-5 cm depth) samples of each wildfire-burnt site (B1, B2, and B3).

Classification	Burn severity level	MTR °C	B1		B2		B3	
			0-2 cm	2-5 cm	0-2 cm	2-5 cm	0-2 cm	2-5 cm
Unburned	0	<40	-	-	-	-	-	-
Low	1	40 - 100	-	IV	-	5	-	-
Moderate	2	100 - 200	-	-	5 ; 7	1 ; 2 ; 3 ; 4 ; 7 ; 8 ; 9 ; 10	$\delta ; \gamma$	$\beta ; \gamma ; \delta$
	3	200 - 300	IV	I ; II ; V	2	6	ϵ	$\alpha ; \epsilon$
	4	300 - 400	I ; III ; V	III	1 ; 3 ; 4 ; 8 ; 9 ; 10	-	$\alpha ; \beta$	-
High	5	400 - 500	II	-	6	-	-	-
Very high	6	> 500	-	-	-	-	-	-

In Maia et al., (2012) study top-soil samples (0-3 cm depth) were collected in a area with similar characteristics as in the present study, having as main vegetation types maritime pine (*Pinus pinaster*) and eucalypt (*Eucalyptus globulus*), and schist as parent rock. As mentioned before, the MTR estimations in this study ranged between 53°C and 125°C, which are quite lower values than the ones registered in the present work.

2.4 CONCLUSIONS

The principal aim of this work was to assess how spatial variability in soil properties affected the accuracy of NIR-based predictions of the maximum temperatures reached (MTR) by heating soils under controlled laboratory conditions. One advantage of using NIR spectroscopy is to be time-saving. In this sense, the number of samples for laboratory analyses, and data processing (to perform the calibrations) needs to be kept to a minimum. Furthermore, the time frame available for soil spectra to reflect soil temperatures after a fire event can be quite limited, either due to erosion or human activity (Guerrero et al., 2007; Lugassi et al., 2010), thus the number of field samples to be collected need also to be kept to a minimum. However, so that to perform good and trustworthy estimations, models require limited but sufficient heterogeneity (Cecillon et al., 2009), what in this work is referred as variability. One of the two long-unburnt study sites revealed marked variability over distances as short as 5 meters, whereas the other did not. In the former case, especially the MTR predictions by the models underpinned by a single soil sample were not reliable, since the accuracy of these predictions depended strongly from model to model. The models based on larger sample numbers, however, provided robust MTR predictions, even when these models involved samples from the two study sites. This probably reflected the sites comparable parent materials, soils and land cover (eucalypt plantations). In general, models involving a more heterogeneous set of samples should be less sensitive to deviant samples but, at the same time, less accurate for “typical” samples. Further work is needed to provide more insight in this trade-off, especially so that the method can be used on a routinely basis for assessing burn severity after wildfires. Nonetheless, the present results suggested that the *Mahalanobis* distance is a suitable indicator of whether the MTR of a specific wildfire-burnt sample can be estimated by a certain model with acceptable accuracy.

CHAPTER 3 – THE APPLICABILITY OF NEAR-INFRARED SPECTROSCOPY IN THE STUDY OF SOILS

A recent review by Cecillon and Brun (2010) has demonstrated that near-infrared reflectance spectra contain much information related to soil quality, and that good predictions can be achieved for many chemical and some physical and biological properties involved in soil conditions. The advantages offered by this technique include:

- minimal sample preparation (air drying and sieving) (Arcenegui et al., 2010)
- possibility of simultaneous determination of several constituents in a large number of samples (Ben-Dor and Banin, 2005; Viscarra Rossel et al., 2006)
- a short turnaround time at the laboratory and the need for only basic buildings and the minimal training of staff (Batenn, 1998)

For this reasons it is a fast, low-cost and environmental friendly technique for soil quality monitoring.

The present research revealed that building NIR-based local models is perfectly possible and viable on performing estimations of an important parameter that affects soil quality that is: the maximum temperatures reached by soil recently affected by fire.

Soil NIR spectra can be used as an integrated measure of soil quality, so as to classify sites according to their global degradation status or for monitoring the effect of an ecological factor on soil quality (Cecillon and Brun, 2010), such as the effect of wildfires.

Cecillon and Brun (2010) stressed for the urgent research need for the development of international soil spectral libraries that would improve the predictive ability of NIR for soil quality attributes whatever the soil type. This implies the generalization of local models that contain the NIR-identified soil variability of the different regions in Europe. As we have seen soil variability can be quite large in a matter of meters, thus to build libraries with the extension of countries will certainly be a big challenge. However, if the spectra libraries depend on the parameter of interest as for example, areas classified as sensitive to the risks arising from the occurrence of wildfires, the number of samples required for this library is expected to decrease substantially.

References

AFN (National Forestry Authority), 2010. Annual Report of Burnt Areas and Events. Prepared by the Portuguese Unit Directorate of Forest Protection. <http://www.icnf.pt/portal>. Last time viewed October, 2012.

Almendros, G., González-Vila, F.J. y Martín, F., 1990. Fire-induced transformation of soil organic matter from an oak forest: an experimental approach to the effects of fire on humic substances. *Soil Science*, 149, 158-168.

Almendros, G., Martín, F. y González-Vila, F.J. 1988. Effects of fire on humic and lipid fractions in a Dystric Xerochrept in Spain. *Geoderma*, 42, 115-127.

Almendros, G., Polo, A., Lobo, M.C. y Ibáñez, J.J., 1984. Contribución al estudio de los incendios forestales en las características de la materia orgánica del suelo. II. Transformaciones controladas del humus por ignición en condiciones de laboratorio. *Révue d'Ecologie et Biologie du Sol*, 21, 145-160.

Arcenegui, V., Mataix-Solera, J., Zornoza, R., Pérez-Bejarano, a., Mataix-Beneyto, J., & Gómez, I. (2010). Estimation of the maximum temperature reached in burned soils using near-infrared spectroscopy: Effects of soil sample pre-treatments. *Geoderma*, 158(1-2), 85–92.

Arcenegui, V., Guerrero, C., Mataix-Solera, J., Mataix-Beneyto, J., Zornoza, R., Morales, J. y Mayoral, A.M., 2008. The presence of ash as an interference factor in the estimation of the maximum temperature reached in burned soils using near-infrared spectroscopy (NIR). *Catena*, 74, 177-184.

Batten G. D., 1998. An appreciation of the contribution of NIR to agriculture. *Journal of Near Infrared Spectroscopy* 6, 105–114.

Ben-Dor, E. and Banin, A. 1995. Near-infrared analysis as a rapid method to simultaneously evaluate several soil properties. *Soil Science Society of America Journal*, 59, 364-372.)

Blanco, M., y Villarroya, I., 2002. NIR spectroscopy: a rapid-response analytical tool. *TrAC Trends in Analytical Chemistry*, 21, 240-250.

Bowman, D.M.J.S.; Balch, J.K.; Artaxo, P. Bond, W.J.; Carlson, J.M.; Cochrane, M.S.; D'Antonio, C.M.; DeFries, R.S.; Doyle, J.C.; Harrison, S.P.; Johnston, F.H.; Keeley, J.E.; Krawchuk, M.A.; Kull, C.A.; Marston, B.J.; Moritz, M.A.; Prentice, I.C.; Roos, C.I.; Scott, A.C.; Swetnam, T.W.; van der Werf, G.R.; Pyne, S.J. 2009. Fire in the Earth System. *Science*. 324:481-484.

Burns, D.A. and Ciurczack, E.W. 2001. *Handbook of Near-Infrared Analysis*. Marcel Dekker, New York.

Chang, C., Laird, D. A., Mausbach, M. J., & Hurburgh, C. R., 2001. Near-Infrared Reflectance Spectroscopy–Principal Components Regression Analyses of Soil Properties. *Soil Sci. Soc. Am. J.* 65:480–490

Carroll, E.M., Miller, W.W., Johnson, D.W., Saito, L., Qualls, R.G., Walker, R.F., 2007. Spatial analysis of a large magnitude erosion event following a Sierran wildfire. *Journal of Environmental Quality* 36, 1105–1111.

Cécillon, L. and Brun, J.J., 2010. Near-infrared reflectance spectroscopy (NIRS): a practical tool for the assessment of soil carbon and nitrogen budget. In: Jandl R and Olsson M (eds), COST Action 639, BFW, Vienna, pp. 103-110

Cécillon L., Barthès B.G., Gomez C., Ertlen D., Genot V., Hedde M., Stevens A., Brun J.J., 2009. Assessment and monitoring of soil quality using near infrared reflectance spectroscopy (NIRS). *European Journal of Soil Science* 60: 770-784

Certini, G. 2005. Effects of fire on properties of forest soils: a review. *Oecologia*, 143, 1-10.

Cocke, A. E., Fulé, P. Z., and Crouse, J. E., 2005. Comparison of burn severity assessments using Differenced Normalized Burn Ratio and ground data. *International Journal of Wildland Fire*, 14(2), 189. doi:10.1071/WF04010

Coelho, C.O.A., Ferreira, A.J.D., Boulet, A.K., Keizer, J.J., 2004. Overland flow generation processes, erosion yields and solute loss following different intensity fires. *Quarterly Journal of Engineering Geology and Hydrogeology* 37, 233–240.

De Santis, A. and Chuvieco, E., 2007. Burn severity estimation from remotely sensed data: Performance of simulation versus empirical models. *Remote Sensing of Environment*, 108, 422–435.

DRA-Centre (2002). Vouga River Basin Plan, Phase 1, Analysis and diagnosis of the reference situation . Biophysics analysis, Attachments. Center Regional Directorate of the Environmental. Lisbon, Portugal.

Dunn, B.W., H.G. Beecher, G.D. Batten, and S. Ciavarella. 2002. The potential of near-infrared reflectance spectroscopy for soil analysis—A case study from the Riverine Plain of south-eastern Australia. *Aust. J. Exp. Agric.* 42:607–614.

Díaz-Delgado, R., Lloret, F., & Pons, X., 2003. Influence of fire severity on plant regeneration by means of remote sensing imagery. *International Journal of Remote Sensing*, 24, 1751–1763.

Doerr, S.H., Woods, S.W., Martin, D.A., Casimiro, M., 2009. 'Natural background' soil water repellency in conifer forests of the north-western USA: its prediction and relationship to wildfire occurrence. *Journal of Hydrology* 371, 12–21.

Doerr, S.H.; Shakesby, R.A.; Blake, W.H.; Chafer, C.J.; Humphreys, G.S.; Walbrink, P.J. 2006. Effects of differing wildfire severities on soil wettability and implications for hydrological response. *Journal of Hydrology*. 319: 295-311.

Doerr S.H., Shakesby R.A., Walsh R.P.D., 2000. Soil water repellence: its causes, characteristics and hydro-geomorphological significance. *Earth-Sci Rev* 51:33–65

Fernández, I., Cabaneiro, A. y Carballas, T., 2001. Thermal resistance to high temperatures of different organic fractions from soils under pine forest. *Geoderma*, 104, 281-298.

Fritze, H., Järvinen, P. y Hiukka, R. 1994. Near-infrared characteristics of forest humus are correlated with soil respiration and microbial biomass in burnt soil. *Biology and Fertility of Soils*, 18, 80-82.

Ferreira, A.J.D., Coelho, C.O.A., Boulet, A.K., Lopes, F.P., 2005. Temporal patterns of solute loss following wildfires in Central Portugal. *International Journal of Wildland Fire* 14, 401–412.

Ferreira, A.J.D., Coelho, C.O.A., Ritsema, C.J., Boulet, A.K., Keizer, J.J., 2008. Soil and water degradation processes in burned areas: lessons learned from a nested approach. *Catena* 74, 273–285.

Fritze, H., Järvinen, P. y Hiukka, R., 1994. Near-infrared characteristics of forest humus are correlated with soil respiration and microbial biomass in burnt soil. *Biology and Fertility of Soils*, 18, 80-82.

Gabet, E.J., 2003. Post-fire thin debris flows: sediment transport and numerical modelling. *Earth Surface Processes and Landforms* 28, 1341–1348.

GFA - Global Forest Resources Assessment. Main Report, 2010. FAO - Food and Agriculture Organization of the United Nations.

Giovannini, G., Lucchesi, S., Giachetti, M., 1988. Effect of heating on some physical and chemical parameters related to soil aggregation and erodibility. *Soil Science* 146, 255–262.

González-Pérez, J.A., González-Vila, F.J., Almendros, G., Knicker, H., 2004. The effect of fire on soil organic matter – a review. *Environmental International*, 30, 855-870

Guerrero, C., Mataix-Solera, J., Gómez, I., García-Orenes, F. y Jordán, M.M. 2005. Microbial recolonization and chemical changes in a soil heated at different temperatures. *International Journal of Wildland Fire*, 14, 385-400.

Guerrero, C., Mataix-Solera, J., Arcenegui, V., Mataix-Beneyto, J., Gómez, I., 2007. Near-infrared spectroscopy to estimate the maximum temperatures reached on burned soils. *Soil Science Society of America Journal* 71 (3), 1029–1037.

Imeson A.C., Verstraten J.M., van Mulligen E.J., Sevink J., 1992. The effects of fire and water repellence on infiltration and runoff under Mediterranean type forest. *Catena* 19:345–361

IFN5, 2006. 5th National Forest Inventory Final Report. Institute for Nature Conservation and Forestry (ICNF).

ICNF - Statistics 2001-2010. Source: web portal of the Institute for Nature Conservation and Forestry (ICNF). <http://www.icnf.pt>. Last time viewed October, 2012.

Jain, T. B., Gould, W., Graham, R. T., Pilliod, D. S., Lentile, L. B., & González, G., 2008. A soil burn severity index for understanding soil-fire relations in tropical forests. *Ambio*, 37(7-8), 563-8.

Jain, T. B., 2004. Confused meanings for common fire terminology can lead to fuels mismanagement. A new framework is needed to clarify and communicate the concepts. *Tongue-Tide Wildfire July/August 2004*

Keeley, J.E. 2009. Fire intensity, fire severity and burn severity: a brief review and suggested usage. *International Journal of Wildland Fire*, 18, 116–126.

Keizer, J.J., Doerr, S.H., Malvar, M.C., Prats, S.A., Ferreira, R.S.V., Oñate, M.G., Coelho, C.O.A., Ferreira, A.J.D., 2008. Temporal variation in topsoil water repellency in two recently burnt eucalypt stands in north-central Portugal. *Catena* 74, 192–204.

Lentile, L.; Holden, Z.; Smith, A.; Falkowski, M.; Hudak, A.; Morgan, P.; Lewis, S.; Gessler, P.; Benson, N., 2006. Remote sensing techniques to assess active fire characteristics and post-fire effects. *Int. J. Wildland Fire* 15, 319-345.

Lewis, S.A., J.Q. Wu, and P.R. Robichaud. 2006. Assessing burn severity and comparing soil water repellency, Hayman Fire, Colorado. *Hydrological Processes*, 20, 1-16.

Llovet, J., Ruiz-Valera, M., Josa, R., Vallejo, V.R., 2009. Soil responses to fire in Mediterranean forest landscapes in relation to the previous stage of land abandonment. *International Journal of Wildland Fire* 18, 222–232.

Lugassi, R., Ben-Dor, E., y Eshel, G. 2010. A spectral-based method for reconstructing spatial distributions of soil surface temperature during simulated fire events. *Remote Sensing of Environment*, 114, 322-331

Maia P., Pausas J., Arcenegui V., Guerrero C., Pérez-Bejarano A. Mataix-Solera J., Varela M.E.T., Fernandes I., Pedrosa E.T., Keizer J.J., 2012. Wildfire effects on the soil seed bank of a maritime pine stand — The importance of fire severity. *Geoderma*, 1–9.

Malley, D.F., L. Yesmin, D. Wray, and S. Edwards. 1999. Application of near-infrared spectroscopy in analysis of soil mineral nutrients. *Commun. Soil 1037 Sci. Plant Anal.* 30:999–1012.

Malvar, M.C., Prats, S.A., Nunes, J.P., Keizer, J.J., 2011. Post fire overland flow generation and inter rill erosion under simulated rainfall in two eucalypt stands in north-central Portugal. *Environmental Research* 111, 222–236.

Marcos, E., Tárrega, R. y Luis, E. 2007. Changes in a Humic Cambisol heated (100–500 °C) under laboratory conditions: The significance of heating time. *Geoderma*, 138, 237–243.

Martens, H. y Næs, T. 1989. *Multivariate calibration*. Edita John Wiley and Sons, Chichester, 419 pp

McBratney, A.B., Minasny, B. y Viscarra Rossel, R. 2006. Spectral soil analysis and inference systems: a powerful combination for solving the soil data crisis. *Geoderma*, 136, 272–278.

Miller JD, Yool SR (2002) Mapping forest post-fire canopy consumption in several overstory types using multi-temporal LandsatTMandETMdata. *Remote Sensing of Environment* 82, 481–496. doi:10.1016/S0034-4257 (02)00071-8

Molina M.J. and Llinares J.V. (2001). Temperature–time curves at the soil surface in maquis summer fires. *International Journal of Wildland Fire*, 10, 45–52.

Nasi R., Dennis R., Meijaard E., Applegate G. and Moore P. 2002. Forest fire and biological diversity. *Unasylva* - No. 209 Forest Biological Diversity. An international journal of forestry and forest industries - Vol. 53 - 2002/2. FAO - Food and Agriculture Organization of the United Nations.

Natsuga, M., and Kawamura, S., 2006). Visible and near-infrared reflectance spectroscopy for determining physicochemical proprieties of rice. *American Society of Agricultural and Biological Engineers* 49(4), 1069–1076.

Næs, T., Isaksson, T., Fearn, T. y Davies, T. 2002. *A user-friendly guide to multivariate calibration and classification*. Edita NIR Publications, Chichester, 344 pp.

Neary, D.G., Klopatek, C.C., DeBano, L.F. y Ffolliott, P.F. 1999 Fire effects on belowground sustainability: a review and synthesis. *Forest Ecology and Management*, 122, 51-71.

Neary, D.G., Ryan, K.C., DeBano, L.F., eds. 2005. *Wildland fire in ecosystems: effects of fire on soil and water*. U.S. Forest Service General Technical Report, RMRS-GTR-42-Vol. 4.

Pereira, J. M. C., 1999. A comparative evaluation of NOAA/AVHRR vegetation indexes for burned surface detection and mapping. *IEEE Transactions on Geoscience and Remote Sensing*, 37, 217-226.

Pérez, B., y Moreno, J.M. 1998. Methods for quantifying fire severity in shrubland-fires. *Plant Ecology*, 139, 91-101.

Pietikäinen, J., Hiukka, R. y Fritze, H. 2000. Does short-term heating of forest humus change its properties as a substrate for microbes? *Soil Biology & Biochemistry*, 32, 277-288.

Raison, R.J. 1979 Modifications of the soil environment by vegetation fires, with particular reference to nitrogen transformations: a review. *Plant and Soil*, 51, 73-108.

Russell, C.A. (2003) Sample preparation and prediction of soil organic matter properties by near infra-red reflectance spectroscopy. *Communications in Soil Science and Plant Analysis*, 34, 1557-1572.

Sankey, J.B., Brown, D.J., Bernard, M.L. & Lawrence, R.L. , 2008. Comparing local vs. global visible and near-infrared (VisNIR) diffuse reflectance spectroscopy (DRS) calibrations for the prediction of soil clay, organic C and inorganic C. *Geoderma* 148(2), 149-158.

Shakesby, R.A., 2011. Post-Wildfire soil erosion in the Mediterranean: Review and future research directions. *Earth-Science Reviews* 105, 71-100.

SNIRH - National Information System for Water Resources (Portugal) - 2011 <http://snirh.pt/>. Last time viewed October, 2012.

Sheppard, N., Willis, H.A. & Rigg, J.C. (1985). Names, symbols, definitions and units of quantities in optical spectroscopy. *Pure and Applied Chemistry* 57(1), 105-120.

Shepherd, K.D. & Walsh, M.G. (2002). Development of reflectance spectral libraries for characterization of soil properties. *Soil Sci. Soc. Amer. J.* 66, 988-998.

Terefe, T., Mariscal-Sancho, I., Peregrina, F. y Espejo, R. 2008. Influence of heating on various properties of six Mediterranean soils. A laboratory study. *Geoderma*, 143, 273-280.

van Wageningen, J.W., Root, R.R. y Key, C.H. 2004. Comparison of AVIRIS and Landsat ETM+ detection capabilities for burn severity. *Remote Sensing of Environment*, 92, 397-408.

Veraverbeke, S.; Lhermitte, S.; Verstraeten, W.W.; Goossens, R., 2010. The temporal dimension of differenced Normalized Burn Ratio (dNBR) fire/burn severity studies: The case of the large 2007 Peloponnese wildfires in Greece. *Remote Sens. Environ.* 114, 2548-2563.

Verma, S., & Jayakumar, S. (2012). Impact of forest fire on physical, chemical and biological properties of soil: A review *Proceedings of the International Academy of Ecology and Environmental Sciences*, 2(3):168-176.

Vergnoux, A., Dupuy, N., Guiliano, M., Vennetier, M., Theraulaz, F. y Doumenq, P., 2009. Fire impact on forest soils evaluated using near-infrared spectroscopy and multivariate calibration. *Talanta*, 80, 39–47.

Viscarra Rossel, R.A., Walvoort, D.J.J., McBratney, A.B., Janik, L.J. y Skjemstad, J.O. 2006. Visible, near infrared, mid infrared or combined diffuse reflectance spectroscopy for simultaneous assessment of various soil properties. *Geoderma*, 131, 59-75.

Úbeda, X. and Bernia, S., 2005. The effect of wildfire intensity on soil aggregate stability in the Cadiretes Massif, NE Spain. *Geomorphological Processes and Human Impacts in River Basins* 299, 37–45.

Ulery, L., y Graham, R.C. 1993. Forest fire effects on soil color and texture. *Soil Science Society of America Journal*, 57,135-140.

Wagenbrenner, J.W., MacDonald, L.H., Rough, D., 2006. Effectiveness of three post-fire rehabilitation treatments in the Colorado Front Range. *Hydrological Processes* 20, 2989–3006.

Walter L. and Cressler III., 2001. Evidence of earliest known wildfires. *Palaios*, 16, pp. 171-174

Williams, P. C., & Sobering, D. C. (1993). Comparison of commercial near-infrared transmittance and reflectance instruments for analysis of whole grains and seeds. *Journal of Near Infrared Spectroscopy*, 1,25–32.

Wold, S., Trygg, J., Berglund, A. y Antti, H. 2001. Some recent developments in PLS modelling. *Chemometrics and Intelligent Laboratory Systems*, 58, 131–150.

WRB (World References Base for soil resources), 2006. *World Soil Resources Reports* Nº. 103, 2ª edição. FAO, Rome.

Zornoza, R., Guerrero, C., Mataix-Solera, J., Scow, K.M., Arcenegui, V. y Mataix-Beneyto, J. 2008. Near infrared spectroscopy for determination of various physical, chemical and biochemical properties in Mediterranean soils. *Soil Biology & Biochemistry*, 40, 1923-1930.